Drug Design, Development and Therapy

Dovepress
Taylor & Francis Group

Open Access Full Text Article

ORIGINAL RESEARCH

Integrative Metabolomics and Ionomics Identify Organ-Specific Responses Associated with Cisplatin Treatment in Mice

Rong Sun[1,*], Qin Xiao[2,*], Houlong Long[1], Ruili Dang[3,4], Shiyuan Zhao[3,4], Jinxiu Guo[3,4], Xue Chu[3,4], Haosen Sun[5], Yazhou Zhang[6], Pei Jiang[3,4]

[1]Department of Thyroid and Breast Surgery, Tengzhou Central People's Hospital, Xuzhou Medical University, Tengzhou, 277500, People's Republic of China; [2]Department of Burn and Wound Repair Surgery, Tengzhou Central People's Hospital, Xuzhou Medical University, Tengzhou, 277500, People's Republic of China; [3]Institute of Translational Pharmacy, Jining Medical Research Academy, Jining, 272000, People's Republic of China; [4]Translational Pharmaceutical Laboratory, Jining First People's Hospital, Shandong First Medical University, Jining, 272000, People's Republic of China; [5]Financial Management, Grade 2023, Panhe Campus, Shandong Agricultural University, Taian, 271000, People's Republic of China; [6]Department of Foot and Ankle Surgery, Tengzhou Central People's Hospital,Xuzhou Medical University, Tengzhou, 277500, People's Republic of China

*These authors contributed equally to this work

Correspondence: Yazhou Zhang, Department of Foot and Ankle Surgery, Tengzhou Central People's Hospital, Xuzhou Medical University, Tengzhou, 277500, People's Republic of China, Email jiangnanasia@126.com; Pei Jiang, Translational Pharmaceutical Laboratory, Jining First People's Hospital, Shandong First Medical University, Jining, 272000, People's Republic of China, Email jiangpeicsu@sina.com

Background: Cisplatin is a widely used chemotherapeutic agent effective against various malignant tumors. However, its clinical application is limited by severe toxic side effects on multiple vital organs. Understanding the systemic metabolic and elemental alterations associated with cisplatin is essential for developing strategies to mitigate its toxicity.

Methods: An integrative metabolomics and ionomics approach was employed to investigate organ-specific responses to cisplatin treatment in mice. Gas chromatography-mass spectrometry (GC-MS) and inductively coupled plasma-mass spectrometry (ICP-MS) were used to analyze metabolic and elemental changes in multiple organs, including the heart, liver, spleen, lungs, kidneys, cortex, hippocampus, brown adipose tissue, and blood. Histopathological evaluation was also performed to complement biochemical analyses.

Results: Multivariate statistical analysis indicated that cisplatin was accompanied by significant changes in the levels of several key metabolites, including amino acids, fatty acids, and tricarboxylic acid cycle intermediates. A total of 9 metabolic pathways were implicated, particularly those involved in amino acid biosynthesis, energy metabolism, and redox regulation. In parallel, notable variations in metal ion concentrations, such as Ag, Na, Ca, Zn, Cu, Mg and Fe, were observed across organs. These changes may be linked to alterations in enzyme activity and antioxidant functions.

Conclusion: This study provides a comprehensive overview of metabolic and elemental disturbances in vital organs correlated with cisplatin exposure. The findings suggest that modulation of specific metabolites and trace elements may help reduce cisplatin toxicity. The integrative omics approach offers novel insights into the pathways potentially underlying chemotherapy-induced side effects and highlights possible therapeutic targets.

Keywords: metabolomics, ionomics, cisplatin, organ toxicity

Introduction

Cisplatin (CDDP) is an effective platinum-based chemotherapy drug used to treat a variety of solid tumors,[1,2] including breast, lung, ovarian cancers, and others. CDDP, often referred to as the "penicillin of cancer",[3] exerts its anticancer effects primarily through the formation of DNA adducts, DNA cross-linking, and the induction of apoptosis via oxidative stress and the activation of multiple signaling pathways.[4] Despite its clinical efficacy, CDDP is a platinum-based compound that accumulates in the body and causes dose-limiting side effects, including nephrotoxicity, neurotoxicity,

Received: 22 April 2025
Accepted: 10 September 2025
Published: 22 September 2025

Graphical Abstract

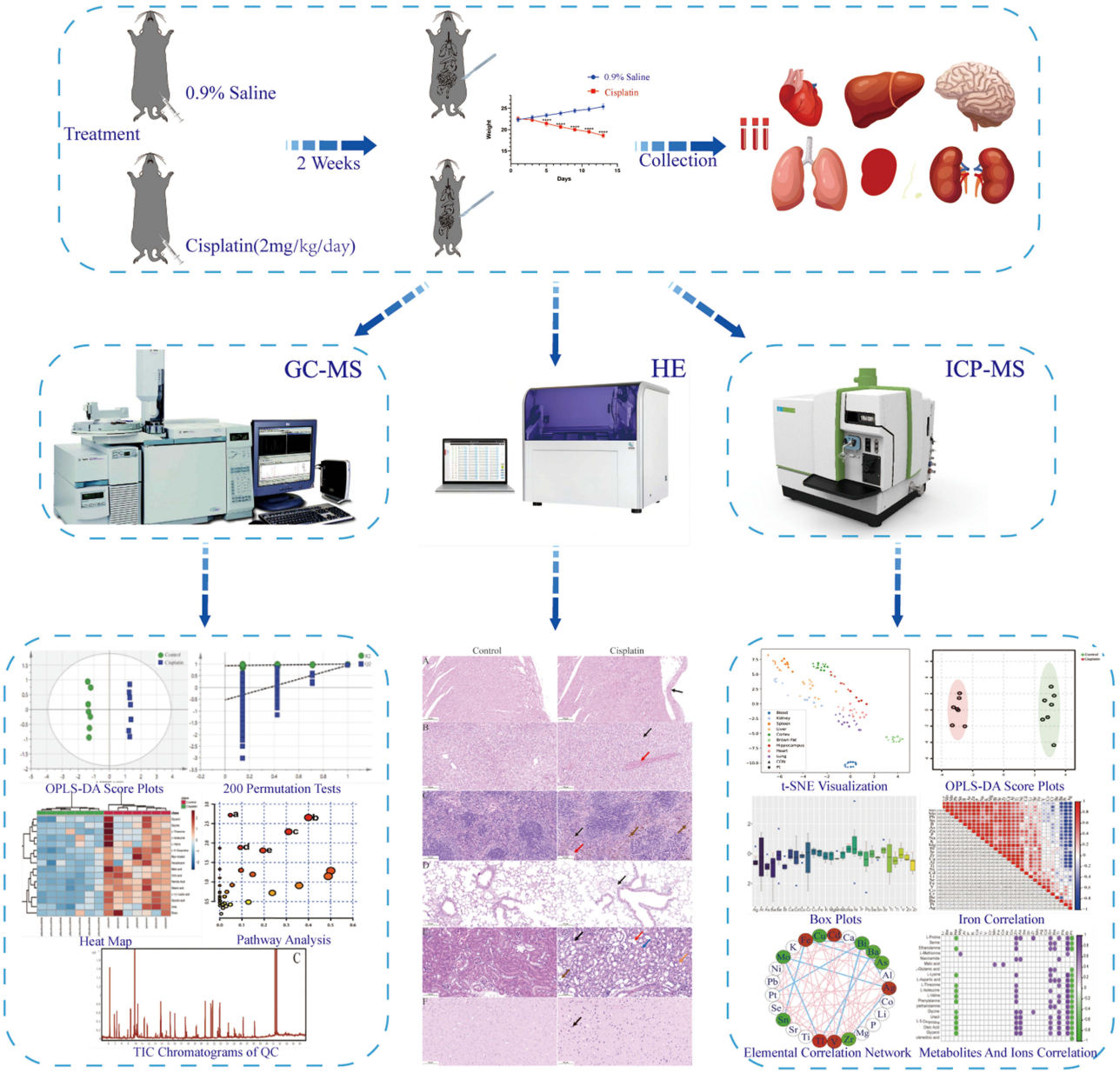

ototoxicity, hepatotoxicity, and cardiotoxicity.[5] These toxicities compromise patients' quality of life, often necessitate dose reduction or treatment interruption, and ultimately hinder therapeutic efficacy. Therefore, CDDP-induced organ toxicity significantly restricts its clinical application. Although CDDP-induced organ toxicity is well recognized, its underlying mechanisms remain incompletely understood. Currently, no effective strategies exist for early diagnosis or prevention, highlighting the urgent need to identify reliable biomarkers and uncover the potential mechanisms underlying cisplatin-induced organ toxicity.

To comprehensively dissect the complex pathophysiological mechanisms of CDDP toxicity across organs, integrative metabolomics and ionomics analysis can provide a more comprehensive understanding. Metabolomics, by profiling

endogenous small molecules, reveals dysregulated metabolic pathways reflecting physiological and pathological states,[6] offering insights into organ-specific metabolic perturbations caused by CDDP. Concurrently, ionomics captures changes in elemental composition and ion homeostasis. Given CDDP's metal-based nature, it likely disrupts the balance of essential ions, contributing to off-target toxicity. Prior studies have linked ionomic changes with various diseases, including inflammation, cancer, cardiovascular disease, and neurodegenerative disorders.[7] For instance, studies have demonstrated that plasma ion spectra serve as an effective tool for evaluating the efficacy of cisplatin-based chemoradiotherapy in cervical cancer patients.[8] In a periodontitis research,[9] ion spectrum changes revealed inflammatory biomarkers; copper (Cu) and selenium (Se) are regarded as specific biomarkers for acute myocardial infarction patients;[10] in osteoarthritis studies,[11] ionomics aids in identifying ion alterations associated with disease progression; in Alzheimer's disease (AD) research,[12] ion spectrum analysis offers novel insights for early diagnosis. However, integrated metabolomic and ionomic profiling across multiple organs in cisplatin-induced toxicity models remains scarce. A holistic understanding integrating metabolite and elemental dysregulation is crucial for elucidating toxicity mechanisms and identifying predictive biomarkers.

In this study, we employed gas chromatography–mass spectrometry (GC–MS) and inductively coupled plasma mass spectrometry (ICP–MS) to analyze metabolic and elemental alterations in multiple organs of cisplatin-treated mice. By integrating statistical analyses and correlation networks, we systematically investigated the organ-specific response to CDDP and the potential interplay between metabolites and ions. Our findings provide novel insights into the mechanisms of cisplatin-induced multi-organ toxicity and offer a basis for future studies aimed at toxicity mitigation.

Materials and Methods

Chemicals and Reagents

Cisplatin was obtained from Shanghai Yuanye Biotechnology Co., Ltd., and 0.9% sodium chloride injection was procured from Shandong Qidu Pharmaceutical Co., Ltd. Heptadecanoic acid, N, O-bis (trimethylsilyl) trifluoroacetamide (BSTFA + 1% TMCS), and multi-element calibration standards (with each element concentration of 100 mg/L) were purchased from Merck. 65% nitric acid (trace analysis grade) was sourced from Thermo Fisher Scientific, and was primarily used for sample digestion and pretreatment to ensure the accuracy and sensitivity of the analysis. Methanol and pyridine (chromatographic grade) were obtained from Shanghai MacLean Biochemical Co., Ltd., and are commonly used in gas and liquid chromatography analyses to provide high-purity solvents that prevent interference. o-Methylhydroxylamine hydrochloride was obtained from Beijing J&K Science Co., Ltd. and used as a derivatization reagent to enhance the detection sensitivity of ketones and aldehydes in the sample. Ultrapure water from Hangzhou Wahaha Company was used for all chemical reagents and sample preparation to ensure the reliability and repeatability of the experimental results.

Animals Treatment

Male C57BL/6J mice, 8 weeks old, weighing 20–25 g, were obtained from Jinan Pengyue Experimental Animal Breeding Co., Ltd. Prior to the experiment, the mice were acclimated for one week to adapt to the experimental environment. Fourteen mice were randomly assigned to two groups: a control group (n=7) and a cisplatin-treated group (n = 7). Each mouse was considered an independent biological replicate. All subsequent analyses, including metabolomics, ionomics, and histopathological assessments, were independently conducted on samples from each individual mouse. No technical replicates were pooled. The sample size was determined based on prior studies and practical feasibility, aiming to ensure sufficient statistical power while minimizing animal use. Unless otherwise specified, all experiments were performed using independent biological replicates (n = 7 per group).

The cisplatin-treated group received intraperitoneal injections of cisplatin (2 mg/kg/day), while the control group received equivalent volumes (0.2 mL) of 0.9% saline. The experiment lasted for two weeks, during which the weight and overall health of the mice were monitored regularly to evaluate the drug's effects on their physiological state. The cisplatin dose and treatment duration were selected based on previous studies and relevant academic literature to ensure the scientific validity and rationale of the experimental design.[13] This repeated low-dose protocol was chosen to model chronic or cumulative toxicity, as it closely mimics the clinical setting of repeated cisplatin administration during chemotherapy.

Similar regimens have been widely employed in previous studies to induce progressive, organ-specific toxicity without causing acute lethality. This study adhered to the guidelines for the care and use of experimental animals issued by the State Science and Technology Commission of the People's Republic of China. The research protocol was approved by the Medical Laboratory Animal Ethics Committee of Jining No.1 People's Hospital (approval number: JNRM-2024-DW-158). We confirm that all methods were reported in accordance with the ARRIVE guidelines (https://arriveguidelines.org).

Sample Collection and Preparation

At the conclusion of the study, all mice were anesthetized with sodium pentobarbital to induce unconsciousness. Subsequently, blood was collected from the portal vein, and the mice were sacrificed by cervical dislocation while unconscious. Serum was then obtained by centrifugation. Dissection was performed in a low-temperature environment to ensure the rapid collection of organs, including the heart, liver, spleen, lungs, kidneys, cerebral cortex, hippocampus, and brown adipose tissue. The collected tissue samples were immediately washed in phosphate-buffered saline (PBS) to remove blood residues, rapidly frozen in liquid nitrogen, and stored at −80°C for subsequent analysis.

Hematoxylin and Eosin (H&E) Staining

Tissue samples were fixed in 4% paraformaldehyde for 24 hours to ensure adequate fixation, followed by dehydration and paraffin embedding with a section thickness of 5 μm. The sections were deparaffinized in xylene to remove residual paraffin. Subsequently, the sections were rehydrated using graded ethanol solutions (100%, 95%, 70%). The sections were then stained with hematoxylin for 5–10 minutes, rinsed, and differentiated with 0.5% hydrochloric acid ethanol to enhance contrast. Following this, the sections were stained with eosin for 2–5 minutes and rinsed. Finally, the sections were dehydrated in 70% ethanol, cleared in xylene, and sealed using neutral resin. The prepared sections were observed under an optical microscope to evaluate changes in tissue morphology and cellular structure.

Metabolomics and GC-MS Analysis

Serum samples (100μL) were mixed with 50μL of 100μg/mL heptadecanoic acid (internal standard) in methanol, vortexed, and centrifuged at 3000 rpm for 10 min at 4°C. The supernatant was evaporated under nitrogen at 37°C. Derivatization was carried out by adding 80μL of methoxyamine hydrochloride in pyridine and incubating at 70°C for 1.5 h, followed by 100μL of BSTFA with 1% TMCS for an additional 1 h. After centrifugation, the supernatant was filtered through a 0.45μm membrane. Tissue samples (~50 mg) were homogenized in methanol, spiked with the same internal standard, and processed similarly. QC samples were prepared by pooling equal aliquots from all samples.

GC-MS analysis was conducted using an Agilent 7890B GC coupled to a 7000C triple quadrupole MS and an HP-5MS column. The oven temperature program started at 60°C (held for 4 min), increased to 300°C at 8°C/min, and was held for 5 min. The injection volume was 1μL, with helium as the carrier gas at 1 mL/min. The inlet, transfer line, and ion source were set at 280°C, 250°C, and 230°C, respectively. Electron ionization (70 eV) was used, and full scan data were acquired over m/z 50–800. QC samples were analyzed every five runs to ensure data quality and instrument stability.

Ionomics and ICP-MS Analysis

Serum (50 μL) or tissue (50 mg) samples were digested with 1 mL of 65% nitric acid at 130 °C for 2 h. All containers were pre-cleaned by soaking in 6 M nitric acid overnight, rinsed with ultrapure water, and air-dried. After cooling, the digested solutions were neutralized and diluted with ultrapure water to the required volume. Elemental analysis was performed using a NexION 1000G ICP–MS (PerkinElmer, USA) equipped with a helium collision cell. Instrumental optimization was conducted prior to measurement. Scandium, germanium, indium, and rhenium (20 μg/L) were used as internal standards and introduced online via a peristaltic pump.

Instrument settings included a nebulizer flow rate of 1.04 L/min, auxiliary gas flow of 1.20 L/min, plasma gas flow of 15 L/min, RF power of 1600 W, analog voltage of –1862 V, and pulse voltage of 1250 V. A total of 35 elements were initially targeted, including Li, Be, B, Na, Mg, Al, Si, P, K, Ca, Ti, V, Cr, Mn, Fe, Co, Ni, Cu, Zn, As, Se, Sr, Zr, Mo, Ag, Cd, Sn, Sb, Ba, Tl, Pb, Bi, Hg, Ir, and Pt. After quality filtering, 31 elements were quantified reliably: Li, Be, Na, Mg, Al, P, K, Ca, Ti, V, Cr, Mn, Fe, Co, Ni, Cu, Zn, As, Se, Sr, Zr, Mo, Ag, Sn, Cd, Sb, Ba, Tl, Pb, Bi, and Pt.

Multivariate Statistical Analyses

We used Agilent Unknowns and MassHunter analysis software (Agilent Technologies, California, USA) to process the acquired GC-MS data. First, chromatographic peaks were extracted from the GC-MS data, and important peaks were identified through signal-to-noise ratio filtering and deconvolution, which enhanced the accuracy of metabolite identification. The resulting mass spectral data were then cross-referenced with the NIST14.0 mass spectral library for metabolite identification. Multivariate statistical analysis was performed on the normalized peak area, corresponding to the proportion of each peak area relative to the total peak area, using SIMCA 14.0 software (Umetrics, Umea, Sweden). Prediction models were constructed using orthogonal partial least squares discriminant analysis (OPLS-DA). Additionally, a two-tailed Student's *t*-test was performed using SPSS 27.0 software to identify metabolites with significant expression differences between groups. In the OPLS-DA model, metabolites with predicted VIP scores greater than 1.0 were prioritized, while metabolites with adjusted p-values (p adjusted) < 0.05 after Benjamini-Hochberg false discovery rate (FDR) correction were considered potential biomarkers. Finally, metabolic pathway analysis was conducted using MetaboAnalyst 6.0 (http://www.metaboanalyst.ca) and the Kyoto Encyclopedia of Genes and Genomes (KEGG; http://www.kegg.jp).

In the ICP-MS data analysis, the k-nearest neighbor algorithm (k-NN) based on Euclidean distance was initially employed to impute missing data. Statistical analyses were conducted using the R programming software package. Differential ions were analyzed using a *t*-test followed by Benjamini-Hochberg FDR correction, and ions with p adjusted < 0.05 were considered significantly changed. Dimensionality reduction and visualization of multivariate organ data were performed using t-distributed stochastic neighbor embedding (t-SNE). Heatmap analysis was carried out using the "ggplot" function in R. Spearman correlation coefficients were calculated to assess the relationship between each element, with a significance threshold of 0.7 used to define significant element correlations. The results were subsequently imported into Cytoscape version 3.10.2 (Cytoscape Consortium, San Diego, California) to construct an element association network.

Results

Clinical Parameters

During the experiment, we systematically monitored both groups of mice, assessing survival status and measuring body weight every two days. Throughout the experiment, the mice in both groups showed no signs of mortality. The weight measurement results indicated no statistically significant difference between the two groups on days 1 and 4. However, on days 5, 7, 9, 11, and 13, a statistically significant difference in body weight was observed ($P < 0.0001$; Figure 1), which may suggest that cisplatin treatment is associated with decreased body weight in mice.

Histopathological Analysis

The morphological effects of cisplatin on the organ tissues of mice were evaluated using hematoxylin-eosin (HE) staining (Figure 2). The control group exhibited normal morphology across all examined tissues, including the heart, liver, spleen, lungs, kidneys, cerebral cortex, hippocampus, and brown fat. These tissues displayed uniform staining, with no evident necrosis or inflammatory cell infiltration. In contrast, the cisplatin-treated group exhibited diverse morphological alterations. Specifically, the heart tissue exhibited a thin right ventricular wall (black arrow). In the liver tissue, the boundaries of the liver lobules were indistinct, with numerous edematous hepatocytes (green arrow). The cells appeared swollen, with loose and lightly stained cytoplasm, and rare venous congestion (red arrow). The spleen exhibited a reduced number of local white pulps with irregular shapes. The red pulp consisted of splenic cords and sinusoids, with focal edema, a small number of granulocytes, and slightly dilated splenic sinusoids (purple arrows). White blood cells were observed in the sinusoids, along with increased brown pigment deposition in both the red and white pulps (brown arrows). In the lung tissue, a small number of alveoli were slightly dilated, with occasional perivascular edema (gray arrows) and loose surrounding connective tissue. Minimal lymphocyte infiltration and vascular congestion were also observed. In the renal cortex, the glomeruli were evenly distributed, with numerous dilated tubules of irregular shapes and flattened tubular epithelial cells. A small number of atrophic tubules, small tubules, and tubular epithelial cells with

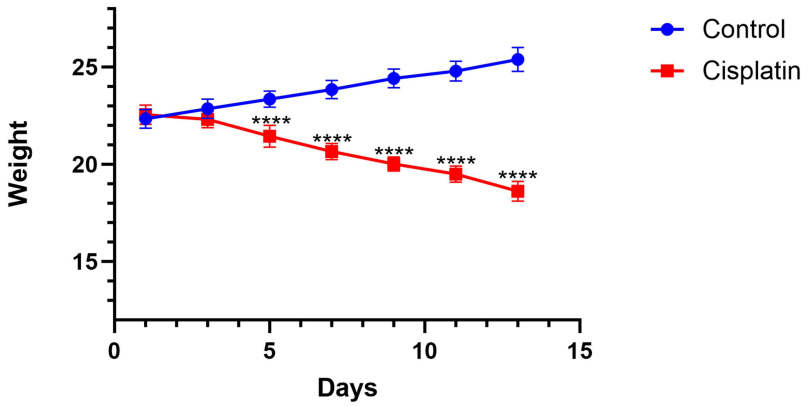

Figure 1 Effect of cisplatin on body weight in mice. Mice were intraperitoneally administered cisplatin (2 mg/kg/day; n = 7) or vehicle (control; n = 7) once daily for 14 consecutive days. Body weight was recorded every 2 days throughout the experiment. Cisplatin-treated mice exhibited a significant reduction in body weight compared to the control group starting from day 5 (****P < 0.0001; Student's *t*-test). Data are presented as mean ± SEM.

watery degeneration (orange arrows) were observed. The cytoplasm appeared loose and lightly stained, with occasional detached epithelial cells in the tubular cavity (yellow arrows), rare eosinophilic substances, and tubular protein casts (blue arrows). No significant abnormalities were noted in the medulla. In the cerebral cortex, abundant neurons were observed, with a small number exhibiting wrinkled and dark staining (pink arrows). These cells appeared shrunken and degenerated, with unclear nuclear cytoplasm.

Metabolomic Analysis

GC-MS Total Ion Chromatograms of Serum and Various Organ Tissues

Figure S1 presents representative GC-MS total ion chromatograms (TICs) of QC samples from serum and various organ tissues, which provide a robust foundation for both qualitative and quantitative metabolite analysis. The TICs of the various QC samples displayed significant differences. The signal intensities of all samples were substantial, indicating high detection sensitivity. A substantial number of metabolites were successfully detected during instrument operation, and significant peak intensities were observed. The high consistency in retention times across different samples suggest excellent spectral resolution and reproducibility of this analytical technique.

Utilization of OPLS-DA for Metabolic Differentiation

This study employed orthogonal partial least squares discriminant analysis (OPLS-DA) to analyze the metabolic data from the two groups, resulting in a clear separation between the sample groups and suggesting the presence of notable metabolic differences. Additionally, the minimal within-group variability supports the consistency and reliability of the experimental approach. As shown in Table 1, all model metrics exceeded 0.5 and were close to 1, indicating high fit and predictive power. Figure S2 demonstrates that in the permutation test, the intercept of the Q^2 regression line on the y-axis is less than zero, and the Q^2 values of the random model (on the left) are lower than those of the original model (on the right), which supports the conclusion that the model is not overfitted and exhibits high robustness and reliability.

Tissue Metabolite Cluster Analysis

Cluster analysis of tissue metabolites suggested that samples were separated into two distinct clusters based on intervention conditions (control group and cisplatin-treated group) (Figure 3). Despite slight overlap between the two groups, most samples from the control and cisplatin-treated groups clustered distinctly within their respective groups. Significant differences in metabolite levels were observed between the two groups, whereas intra-group variations were relatively minor. Moreover, minimal variations in metabolite levels within each cluster further validated the model's discriminatory capability and stability.

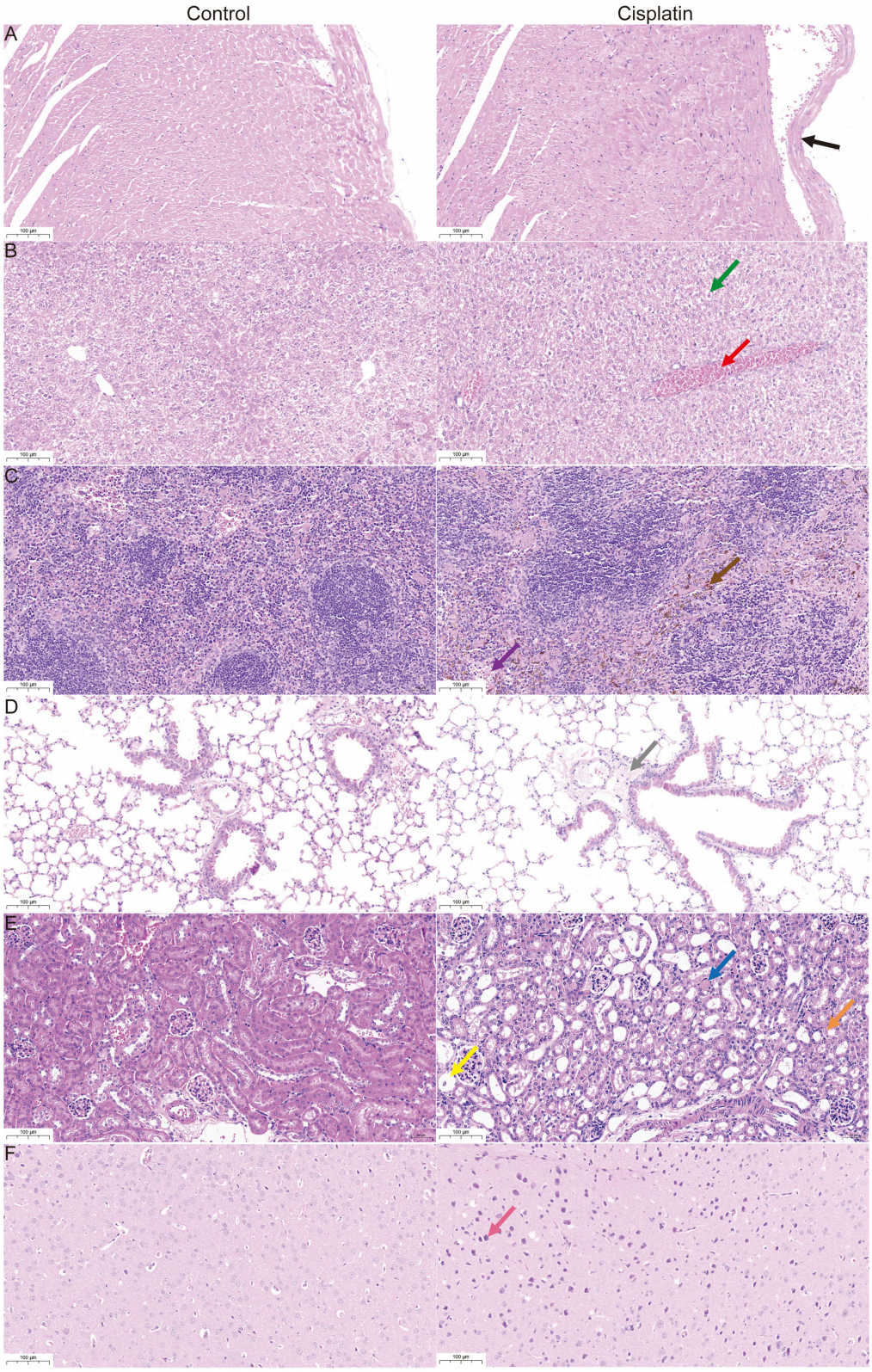

Figure 2 Histopathological Results of Hematoxylin-Eosin (HE) Staining: Comparison of Organ Tissues Between Control and Cisplatin-Treated Mice (**A**) Heart, (**B**) Liver, (**C**) Spleen, (**D**) Lung, (**E**) Kidney, and (**F**) Cerebral cortex. Arrow color indicates lesion type. Black: thin right ventricular wall (heart); Green: edematous hepatocytes with indistinct lobular boundaries (liver); Red: venous congestion (liver); Purple: irregular white pulps (spleen); Brown: pigment deposition (spleen); Gray: perivascular edema (lungs); Orange: tubular epithelial cell degeneration (renal cortex); Yellow: detached tubular epithelial cells (renal cortex); Blue: tubular protein casts (renal cortex); Pink: degenerated neurons (cerebral cortex). Scale bars: 100 μm.

https://doi.org/10.2147/DDDT.S531720

Table 1 The OPLS-DA Parameters in Target Organ Tissues

Tissue	R2X (cum)	R2Y (cum)	Q2 (cum)
Heart	0.608	0.986	0.768
Liver	0.719	0.982	0.875
Spleen	0.710	0.998	0.947
Lung	0.660	0.999	0.888
Kidney	0.555	0.999	0.786
Cerebral cortex	0.730	1.000	0.767
Hippocampus	0.577	0.999	0.878
Brown fat	0.585	0.998	0.961
Serum	0.783	1.000	0.954

Differential Metabolites

To comprehensively investigate the metabolic differences between the control and cisplatin-treated groups, detailed metabolite analysis was conducted using SIMCA 14.0 and SPSS 27.0 software. The criteria for selecting differential metabolites were VIP values greater than 1.0 and P adjusted less than 0.05. The analysis identified 58 metabolites with significant differences between the control and cisplatin-treated groups, primarily in major organ tissues such as the heart, liver, spleen, lung, kidney, cerebral cortex, hippocampus, brown fat, and serum. These metabolite changes may be associated with the effects of cisplatin treatment on metabolic pathways in mice, potentially providing insights into the molecular processes involved in cisplatin toxicity. Table 2 provides a detailed summary of the main metabolite changes, which may serve as a basis for further exploration of biomarkers and the metabolic responses related to cisplatin treatment.

Metabolic Pathway Analysis

MetaboAnalyst 6.0 was employed to perform metabolic pathway analysis of the differential metabolites between the two groups (Figure 4 and Table 3). The results suggested that 9 pathways across multiple organs were significantly altered following cisplatin treatment. The disrupted pathways are mainly centered on amino acid metabolism and its derivatives, suggesting a shared mechanism involving oxidative stress, neurotransmission, and cellular energy regulation.

Ionomics Analysis

Methodological Validation

Under the set instrument working conditions, a mixed standard solution of multiple metal elements was employed as the sample for analysis. The instrument signal response ratio relative to the internal standard signal was plotted against the mass concentration on the x-axis to generate the standard curve (Figure S3). All elements exhibited a strong linear correlation, with a correlation coefficient greater than 0.99. The method's quantitative limit ranged from 0.001 to 48.428 μg/L, and the concentrations of all tested elements fell within this range, demonstrating the instrument's high sensitivity. The recovery rate ranged from 86.9% to 110.5% (Table 4), with accuracy deemed satisfactory; the coefficient of variation (CV) was below 15% (Table 4), indicating good repeatability of the method.

Statistical Analysis

The *t*-test was used to evaluate the differences in ion levels between the control group and the cisplatin-treated group, with a significance level of P adjusted < 0.05. Figure 5 illustrates the analysis of 29 elements across 8 organ tissues and serum. A comprehensive analysis of ion distributions in the organs of both groups of mice using t-SNE visualization revealed distinct clusters primarily composed of tissue-specific ion profiles. Significant differences were observed between the two groups, especially in blood and brown adipose tissue, when compared to other organs. The control and cisplatin-treated groups of the kidney, spleen, and lung exhibited clear separation, while those of the cortex, hippocampus, and heart tissue overlapped (Figure 5). Additionally, OPLS-DA analysis of the organs from both groups of mice revealed significant differences in elemental composition (Figure 6). The specific model parameters are shown in Figure 7, which demonstrates that ion homeostasis in multiple organs was significantly disrupted due to cisplatin exposure.

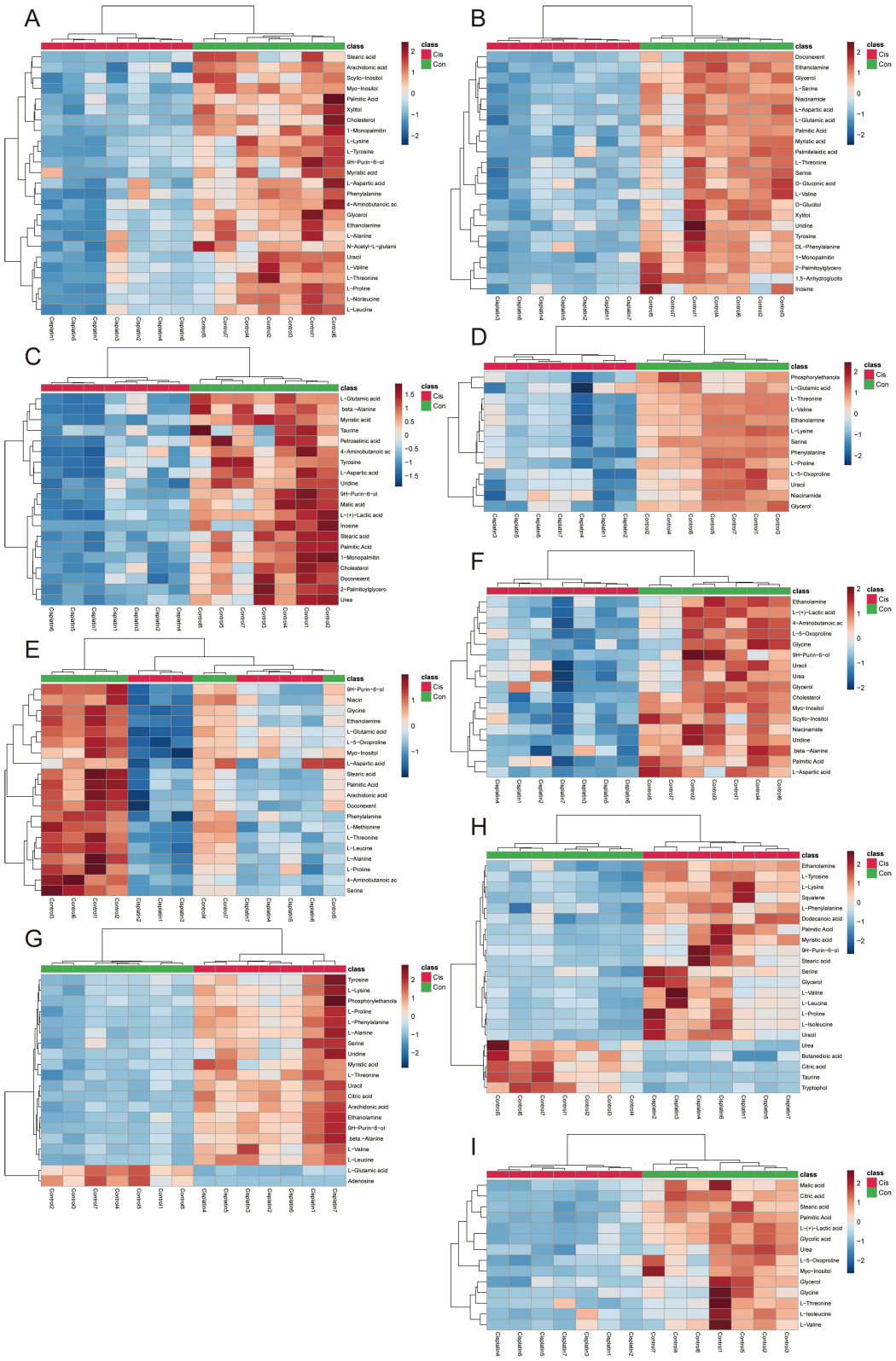

Figure 3 Heatmap visualization of differential metabolites identified in (**A**) Heart, (**B**) Liver, (**C**) Spleen, (**D**) Lung, (**E**) Kidney, (**F**) Cerebral cortex, (**G**) Hippocampus, (**H**) Brown fat, and (**I**) Serum samples between cisplatin-treated and control mice. The columns represent individual samples, and the rows correspond to specific metabolites. Metabolites were selected based on the top 25 features ranked by adjusted p-value (P adjusted < 0.05). The color scale indicates the relative abundance of each metabolite (red: upregulation; blue: downregulation).

https://doi.org/10.2147/DDDT.S531720

https://doi.org/10.2147/DDDT.S531720

Table 2 List of Altered Metabolites in Heart, Liver, Spleen, Lung, Kidney, Cerebral Cortex, Hippocampus, Brown Fat, and Serum Following Cisplatin Exposure

Metabolite	HMDB	Heart		Liver		Spleen		Lung		Kidney		Cerebral Cortex		Hippocampus		Brown Fat		Serum	
		VIP	FC	VIP	FC	VIP	FC	VIP	FC	VIP	FC	VIP	FC	VIP	FC	VIP	FC	VIP	FC
Ethanolamine	HMDB0000149	1.4125	0.38174	1.2348	4.7704E-06			1.9398	7.5698E-05	1.7541	0.000103925	1.4654	0.00029955	1.64292	0.0001033	1.2422	6.2631E-06		
Palmitic Acid	HMDB0000220	1.0997	0.53411	1.0125	5.8462E-07	1.2821	4.7872E-06			1.1293	0.000602762	1.0387	0.00037732			1.2234	0.00153349	1.3460	5.7500E-07
9H-Purin-6-ol	HMDB0000157	1.2305	0.44792			1.3028	2.7836E-05			1.5953	1.5565e-005	1.0978	0.00543321	2.13781	2.8545E-05	1.1434	0.0234981		
Glycerol	HMDB0000131	1.1170	0.55622	1.2397	3.0333E-07			1.2902	1.8385E-05			1.0625	0.00484103	0.23015	0.568041	1.3779	0.00398536	1.0180	0.00303664
L-Threonine	HMDB0000167	1.0954	0.54035	1.0842	0.00019967			1.9547	1.0699E-05	1.6339	0.000135117			1.4706	3.9459E-05			1.0510	0.0154368
Stearic acid	HMDB0000827	1.3652	0.37999			1.0299	8.2932E-05			1.2597	0.000279507					1.2460	0.00353172	1.1294	1.0768E-05
L-Proline	HMDB0000162	1.3629	0.41909					2.2266	1.4228E-05	1.5377	0.00359307			1.66271	3.0442E-05	1.2504	0.00164835		
Uracil	HMDB0000300	1.1922	0.48221					1.5099	0.00018683			1.0945	0.00237322	2.09297	4.9197E-06	1.5431	0.00090199		
Myristic acid	HMDB0000806	1.0531	0.52513	1.0356	1.2765E-06	1.2851	1.7277E-06							1.16377	0.00038786	1.4170	0.00050645		
Serine	HMDB0000187			1.0764	0.00017294			2.0928	1.3213E-06	1.7073	0.000973406			1.13703	0.00700251	1.0189	0.00427489		
L-Glutamic acid	HMDB0000148			1.0991	3.1844E-05	1.3377	1.3177E-06	1.0295	0.0106111	1.1793	0.00194966			1.47395	1.7255E-05				
L-Lysine	HMDB0000182	1.3908	0.39741					2.2452	1.8009E-05					1.50297	0.00102417	1.5052	2.6283E-05		
4-Aminobutanoic acid	HMDB0000112	1.2962	0.45165			1.0897	0.00057395			1.6463	0.00132302	1.3210	0.00017896						
L-Leucine	HMDB0000687	1.2833	0.43847							1.4491	0.000606563			1.92625	9.0913E-06	1.2242	0.00156817		
L-Valine	HMDB0000883	1.2650	0.43488	1.0060	0.00082610			1.8835	3.5753E-05					1.6667	9.3422E-05	1.1254	0.00516421	1.0945	0.00835194
L-Aspartic acid	HMDB0000191	1.0943	0.52829	1.1846	4.3227E-06	1.0508	0.00013334			1.3204	0.00733524	1.9456	2.7537E-05						
Uridine	HMDB0000296			1.1084	0.00124675	1.5203	4.2347E-06					1.6270	6.8635E-06	1.39652	0.00418506				
Urea	HMDB0000294					1.2181	0.00018573					1.2082	0.0130699			1.1882	0.00206006	1.0112	0.00152231
L-5-Oxoproline	HMDB0000267							1.4216	0.00087290	1.0866	0.00326159	1.3979	0.00051810					1.0206	0.00139827
Myo-Inositol	HMDB0000211	1.3779	0.44824							1.0358	0.00999176	1.3676	5.6592E-06					1.6963	0.00040347
Cholesterol	HMDB0000067	1.325	0.41653			1.1647	0.00025915					1.3402	5.7116E-07						
1-Monopalmitin	HMDB0011564	1.3016	0.44288	1.1738	1.8675E-06	1.2029	4.2379E-05												
Phenylalanine	HMDB0000159	1.1655	0.50869					1.7080	8.43382E-0	1.2407	0.00132317								
Niacinamide	HMDB0001406			1.1938	1.7800E-06			1.0738	0.0080055			1.5558	6.3920E-05						
Tyrosine	HMDB0000158			1.2444	1.8033E-05	1.1011	0.00073175							1.36331	0.00652301				
Doconexent	HMDB0002183			1.0016	3.4876E-05	1.2884	0.00011176			1.4195	8.7526e-005								
beta.-Alanine	HMDB0000056					1.1128	9.3181E-05					1.2238	0.00107926	1.80157	0.00017896				
Glycine	HMDB0000123									1.4581	0.000262648	1.3286	0.00280989					1.1200	0.0172852
Citric acid	HMDB0000094													2.15146	2.1906E-07	1.6762	6.9689E-05	1.5999	8.8431E-06
L-Tyrosine	HMDB0000158	1.4054	0.38419													1.3202	1.6422E-05		
Xylitol	HMDB0242149	1.3684	0.39332	1.0951	0.00050415														
L-Alanine	HMDB0000161	1.1702	0.48928							1.5907	0.000432417			1.59937	0.00012332				
Scyllo-Inositol	HMDB0006088	1.0826	0.55918									1.2373	0.00031951						
2-Palmitoylglycerol	HMDB0011533			1.3482	1.0112E-06	1.2433	8.6209E-06												
Inosine	HMDB0000195			1.1652	0.00250839	1.6181	0.00069613												
Malic acid	HMDB0000156					1.2138	0.00026499											1.5105	0.00065574
Phosphorylethanolamine	HMDB0000224							1.626	0.00025522					1.18025	0.00483338				
Arachidonic acid	HMDB0001043	1.4800	0.34235							1.7192	0.00065238			1.41328	3.9564E-05				
L-(+)-Lactic acid	HMDB0000190					1.1768	2.7064E-05					1.8304	8.5183E-05					1.5977	3.0577E-06
L-Phenylalanine	HMDB0000159													1.6839	6.5388E-05	1.1749	0.00019972		
L-Isoleucine	HMDB0000172															1.2800	0.00048728	1.0387	0.0132208
L-Norleucine	HMDB0001645	1.4041	0.39834																
N-Acetyl-L-glutamic acid	HMDB0001138	1.1640	0.48020																

L-Serine	HMDB0000187			1.4234	4.8925E-08														
DL-Phenylalanine	HMDB0250791			1.1319	0.00043910														
1,5-Anhydroglucitol	HMDB0002712			1.2797	0.38055														
D-Glucitol	HMDB0000247			1.0543	4.0947E-05														
D-Gluconic acid	HMDB0000625			1.1029	0.00028432														
Palmitelaidic acid	HMDB0012328			1.0749	4.3161E-05														
Taurine	HMDB0000251					1.0738	0.00591307									1.8112	0.00132983		
Petroselinic acid	HMDB0002080					1.1153	0.00095757												
Niacin	HMDB0001406									1.5439	6.2962e-005								
L-Methionine	HMDB0000696									1.9082	6.18021e-00								
Squalene	HMDB0000256															1.5803	8.89141E-0		
Tryptophol	HMDB0003447															1.3781	0.00026286		
Butanedioic acid	HMDB0000254															1.3614	0.00110921		
Dodecanoic acid	HMDB0000638															1.2625	4.6884E-05		
Glycolic acid	HMDB0000115																	1.5978	3.0448E-06

Abbreviations: VIP, variable importance in projection; FC, fold change = Cisplatin/Control.

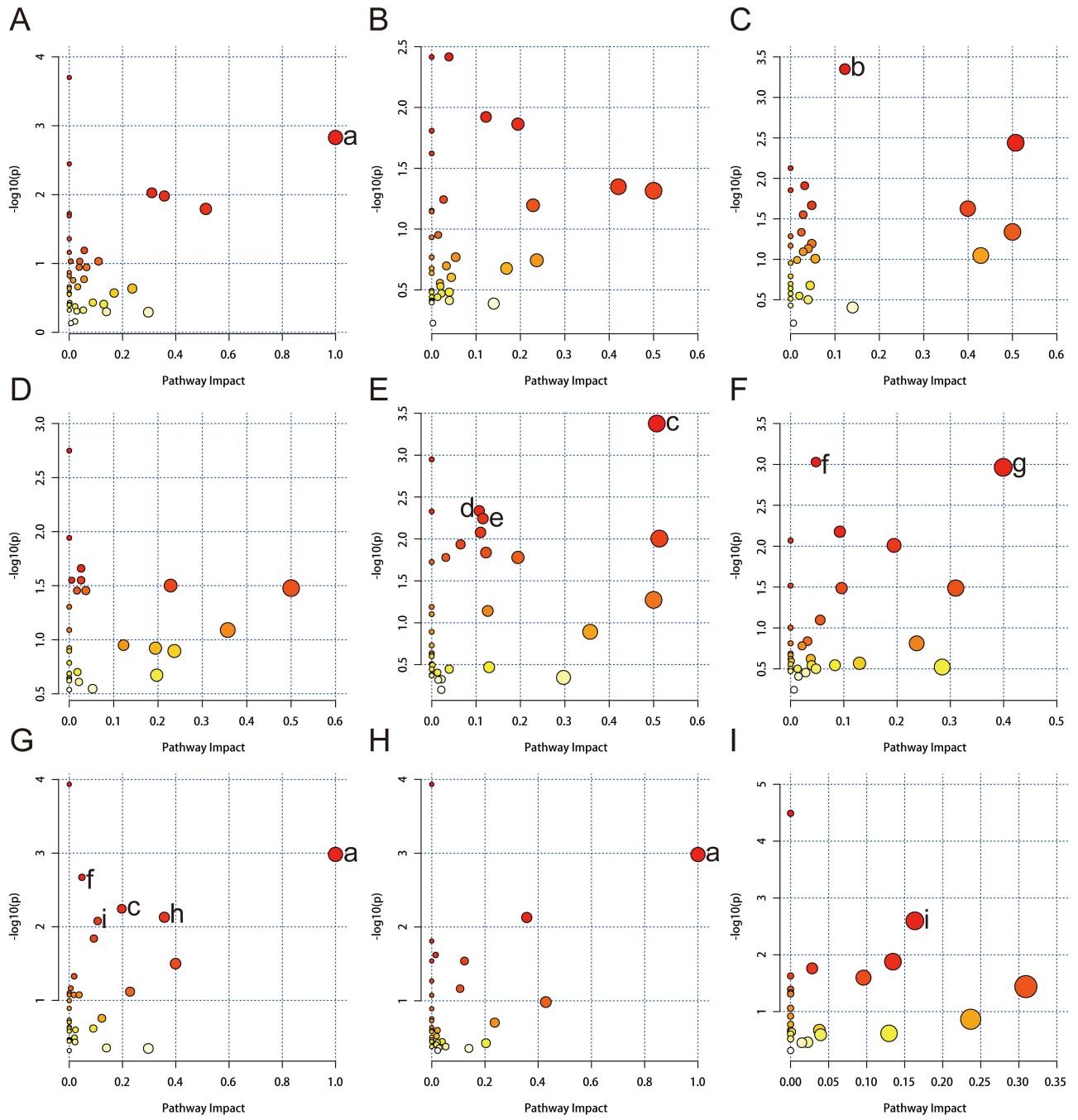

Figure 4 Pathway analysis using MetaboAnalyst 6.0 for (**A**) Heart, (**B**) Liver, (**C**) Spleen, (**D**) Lung, (**E**) Kidney, (**F**) Cerebral cortex, (**G**) Hippocampus,(**H**) Brown fat, and (**I**) Serum. The illustrated pathways include: (a) Phenylalanine, tyrosine and tryptophan biosynthesis; (b) Arginine biosynthesis; (c) Alanine, aspartate and glutamate metabolism; (d) One carbon pool by folate; (e) Glutathione metabolism; (f) Pantothenate and CoA biosynthesis; (g) beta-Alanine metabolism; (h) Phenylalanine metabolism; (i) Glyoxylate and dicarboxylate metabolism.

As shown in Figure 8, Compared to the control group, the Pt content in various tissues of mice in the cisplatin-treated group exhibited varying degrees of increase. Notably, Platinum content in the liver showed the most significant increase, with a fold change of 15,447 compared to the control group. This significant accumulation may be attributed to the liver's role as the primary organ for drug metabolism and detoxification, where its detoxification capacity and high drug transport load make cisplatin and its metabolites prone to retention. In addition, the high affinity of cisplatin to sulfur-containing proteins and the hemodynamic characteristics of the liver may further promote platinum deposition in this organ. Similarly, cisplatin exhibited substantial deposition in the kidneys, consistent with previous studies identifying the

Table 3 Metabolic Pathways Related to the Cisplatin Exposure Intervention Mechanism

Pathway Name	Tissue	Match Status	Hit	P	P Adjusted	Impact
Phenylalanine, tyrosine and tryptophan biosynthesis	Heart	2/4	L-Phenylalanine; L-Tyrosine	0.0014812	0.0318458	1
Arginine biosynthesis	Spleen	3/14	L-Glutamate; L-Aspartate;Urea	0.00052861	0.01638691	0.12234
Alanine, aspartate and glutamate metabolism	Kidney	4/28	L-Aspartate; L-Alanine; L-Glutamate; 4-Aminobutanoate	0.00041973	0.01511028	0.50722
One carbon pool by folate		3/26	Glycine; L-Methionine; L-Serine	0.0046139	0.04112928	0.10714
Glutathione metabolism		3/28	Glycine; L-Glutamate; 5-Oxoproline	0.0057124	0.04112928	0.11548
Pantothenate and CoA biosynthesis	Cerebral cortex	3/20	L-Aspartate; beta-Alanine; Uracil	0.00093595	0.01736	0.04762
Beta-Alanine metabolism		3/21	Beta-Alanine; L-Aspartate; Uracil	0.001085	0.01736	0.39925
Phenylalanine, tyrosine and tryptophan biosynthesis	Hippocampus	2/4	L-Phenylalanine; L-Tyrosine	0.0010405	0.0176885	1
Pantothenate and CoA biosynthesis		3/20	L-Valine; beta-Alanine; Uracil	0.0021325	0.0241683333333333	0.04762
Alanine, aspartate and glutamate metabolism		3/28	L-Alanine; L-Glutamate; Citrate	0.0057124	0.0473189333333333	0.19712
Phenylalanine metabolism		2/10	L-Phenylalanine; L-Tyrosine	0.0074276	0.0473189333333333	0.35714
Glyoxylate and dicarboxylate metabolism		3/32	L-Serine; L-Glutamate; Citrate	0.0083504	0.0473189333333333	0.10667
Phenylalanine, tyrosine and tryptophan biosynthesis	Brown fat	2/4	L-Phenylalanine; L-Tyrosine;	0.0010405	0.01820875	1
Glyoxylate and dicarboxylate metabolism	Serum	3/32	(S)-Malate; Glycine; Citrate	0.0025228	0.031535	0.16333

Table 4 Accuracy and Repeatability of the Measured Trace Elements

Element	Correlation Coefficient (r)	Repeatability Cv [%]	Trueness/ Recovery [%]	Limit of Quantification (μg/L)
Li	0.9999	3.40	98.9	0.006
Na	0.9946	7.72	85.5	6.807
Mg	0.9994	5.57	99.8	0.128
Al	0.9993	5.63	97.1	0.020
P	0.9992	12.78	91.5	0.218
K	0.9995	13.51	82.8	0.893
Ca	0.9989	14.65	94.7	0.974
Ti	0.9999	4.61	83.9	0.008
V	0.9997	4.57	83.1	0.001
Cr	0.9908	4.65	85.6	0.003
Mn	0.9999	4.69	83.2	0.001
Fe	0.9988	4.27	99.2	0.099
Co	0.9998	4.41	84.7	0.001
Ni	0.9968	4.59	83.2	0.005
Cu	0.9999	4.66	91.7	0.010
Zn	0.9975	5.20	89.7	0.044
As	0.9987	4.42	82.1	0.016
Se	0.9998	5.43	82.6	0.029
Sr	0.9797	4.53	81.5	0.003
Zr	0.9980	8.51	92.0	0.002
Mo	0.9998	4.38	85.2	0.001
Ag	0.9992	4.45	87.3	0.002
Cd	0.9999	4.96	81.2	0.001
Sn	0.9979	4.84	81.7	0.001
Sb	0.9998	4.91	81.8	0.001
Ba	0.9754	4.69	81.3	0.013
Pt	0.9999	4.85	88.5	0.001
Pb	0.9985	4.56	82.1	0.001
Bi	0.9998	4.69	83.6	0.001
Tl	0.9997	4.65	83.7	0.001

kidneys as the primary target organ for cisplatin's toxic effects. The order of platinum accumulation across different tissues is as follows: liver > kidney > lung > spleen > heart > brown fat > cortex > hippocampus. This distribution pattern may reflect the exposure and transport characteristics of cisplatin in different organs throughout the body. Furthermore, the cisplatin-treated group showed indications of altered ion balance across multiple organs. Compared to controls, cisplatin exposure was associated with abnormal changes in the concentrations of several elements, including increased Ag levels in multiple tissues, along with shifts in the balance of Na, Ca, Zn, Cu and P. Notably, cisplatin treatment also appeared to affect the concentrations of certain environmental toxic elements, such as As and Tl, in multiple tissues, which may exacerbate cisplatin's toxic effects. These findings indicate a potential disruption of the homeostasis of key biological elements and suggest possible synergistic effects on systemic toxicity through interference with the metabolic pathways of trace elements and toxic metals. Future studies should further investigate the mechanisms underlying these elemental changes and their specific roles in cisplatin-associated toxicity.

To further explore the relationships and trends among ions, we employed the correlation coefficient (r) to quantitatively assess the relationships between elements (Figure 9). Specifically, red represents positive correlations, blue represents negative correlations, and the strength of the correlation is represented by the intensity of the color, where darker colors indicate stronger correlations. In addition, we calculated the Spearman correlation coefficients for all elements in each tissue and constructed an elemental correlation network diagram based on significantly correlated element pairs (Spearman correlation coefficient > 0.70[14]) (Figure 10), a commonly used threshold in omics-based

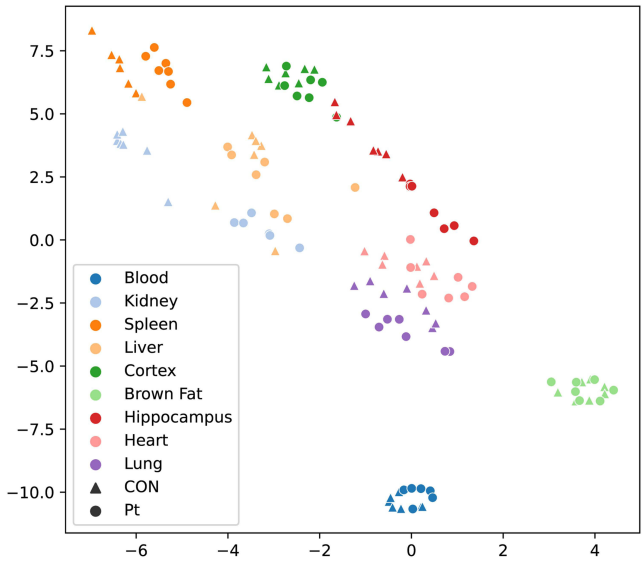

Figure 5 T-SNE visualization of organ-specific feature vectors based on elemental composition.

network studies to indicate strong positive correlations and maintain biological interpretability. We conducted a comprehensive analysis of metabolites and ions in various organs to investigate the correlations between ions and metabolites, as well as their roles in metabolic pathways. As shown in Figure 11, there was a significant correlation between common mineral elements (eg, Ag) and multiple metabolites, the correlation spectra between different ions and metabolites exhibited substantial variability. Under cisplatin exposure, the effect of ion-metabolite interactions on kidney tissue was especially pronounced, followed by liver.

Discussion

Cisplatin is a widely used platinum-based chemotherapy drug for treating a variety of solid tumors. It inhibits cell division by forming DNA cross-links,[15] thereby exerting anti-cancer effects. However, the toxicity resulting from cisplatin's nonspecific effects significantly limits its clinical use, particularly damage to organs such as the liver, kidneys, and central nervous system, representing an urgent challenge. The toxic mechanism of cisplatin is complex and involves ion homeostasis disorders,[16] oxidative stress response,[5] mitochondrial dysfunction,[17] overactivation of inflammatory factors,[18] and substantial damage to several key metabolic pathways.[19] Platinum (Pt), as the core component of cisplatin, is a key cause of multi-organ damage due to its distribution, metabolism, and high affinity for biological molecules in the body. In the kidneys, cisplatin-induced platinum deposition leads to substantial renal dysfunction by activating oxidative stress pathways, inducing acute tubular injury, and upregulating proinflammatory factor expression.[20] In the liver, the accumulation of platinum is closely associated with liver detoxification, drug metabolism, and hemodynamic properties, resulting in cell necrosis, fibrosis, and substantial upregulation of inflammatory factors, indicating that cisplatin exerts a multi-level effect on liver metabolism. Additionally, cisplatin may disrupt core metabolic pathways, such as nucleotide metabolism, amino acid metabolism, sphingolipid metabolism, and glycerophospholipid metabolism, by interfering with the homeostasis of key metal ions and inhibiting the activity of multiple enzymes.[21] Furthermore, cisplatin-induced neurotoxicity in the central nervous system may lead to cognitive dysfunction, memory loss, and behavioral abnormalities by impairing neuronal mitochondrial function, disrupting cellular ion balance, and inducing neuroinflammation. Histological observations indicate that abnormal platinum accumulation in brain tissue threatens the long-term maintenance of neuronal function. This study systematically evaluated the effects of cisplatin exposure on multiple organs, with a particular focus on the toxic mechanisms and potential metabolic regulatory networks in the liver and kidneys, from a comprehensive perspective of metabolism and ion levels. By exploring the interactions between platinum, metabolites, and ions during cisplatin treatment, the study identifies potential associations and regulatory patterns that may serve as biomarkers and targets, providing a critical basis for reducing the toxic side effects of cisplatin in cancer treatment and optimizing chemotherapy strategies.

https://doi.org/10.2147/DDDT.S531720

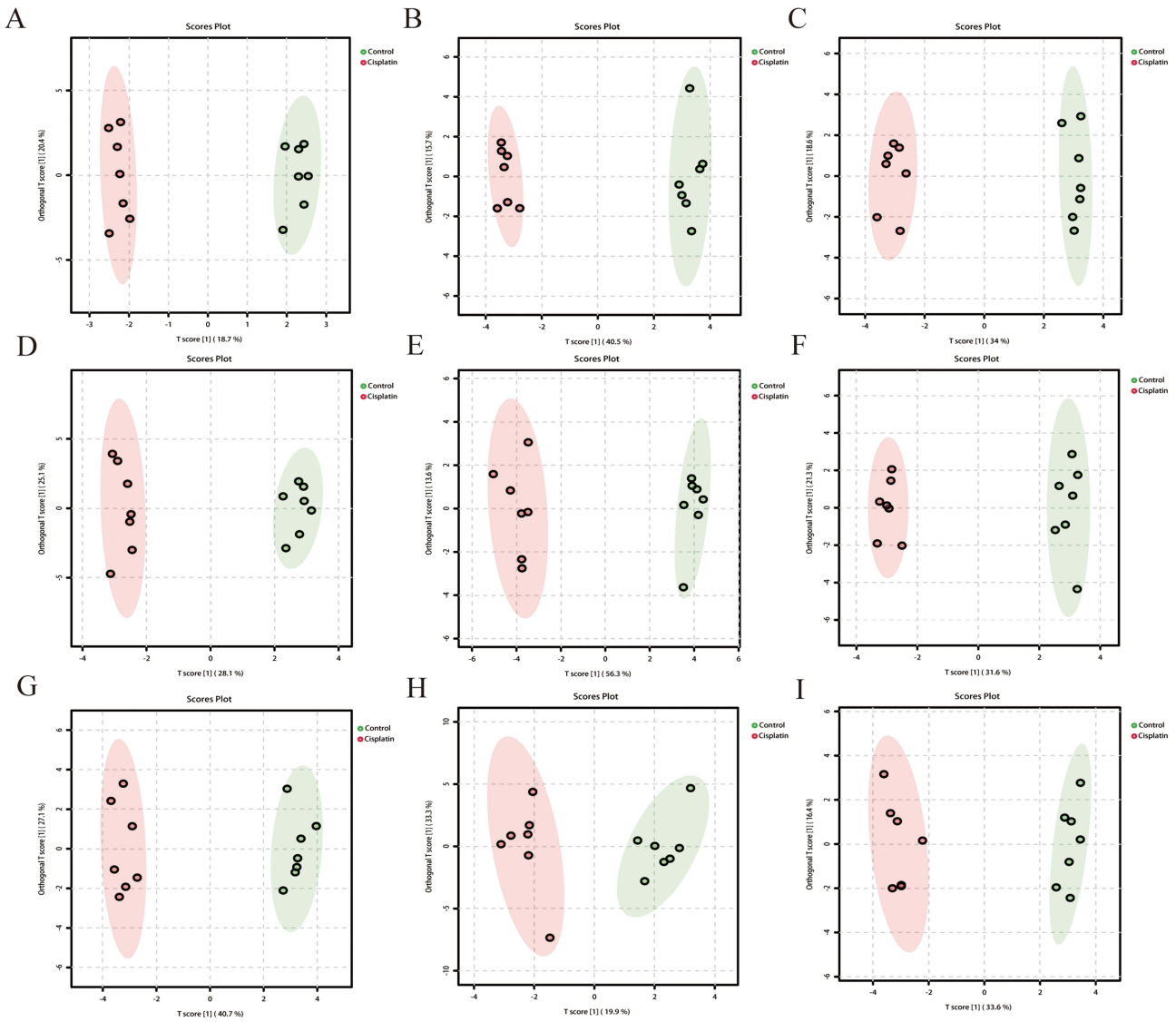

Figure 6 OPLS-DA score plots of ion composition across organs in control and cisplatin-treated mice. (**A**) Heart, (**B**) Liver, (**C**) Spleen, (**D**) Lung, (**E**) Kidney, (**F**) Cerebral cortex, (**G**) Hippocampus,(**H**) Brown fat, and (**I**) Serum.

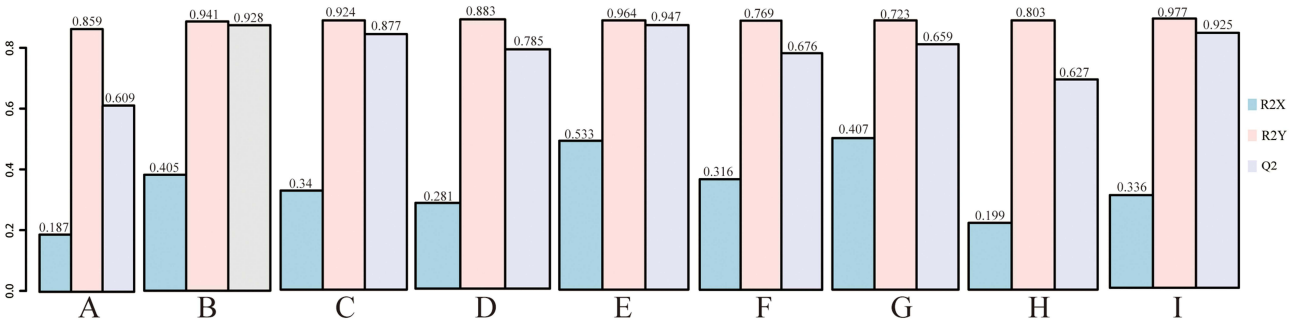

Figure 7 OPLS-DA model parameters for ionomics analysis across organs. (**A**) Heart, (**B**) Liver, (**C**) Spleen, (**D**) Lung, (**E**) Kidney, (**F**) Cerebral cortex, (**G**) Hippocampus, (**H**) Brown fat, and (**I**) Serum.

Differential Metabolite and Metabolic Pathway Analysis

In our study, the levels of L-threonine, glycine, serine, and L-lysine were consistently reduced in multiple organs, suggesting a systemic disruption of amino acid-related metabolic pathways in response to cisplatin exposure. Among them, L-threonine exhibited the most widespread decrease, with significant reductions observed in the heart, liver, lung, kidney, hippocampus, and blood, highlighting its central involvement in cisplatin-induced metabolic alterations. These findings imply that multiple essential physiological functions, such as protein biosynthesis, redox regulation, and neurotransmitter balance, may be affected. As an essential amino acid, L-threonine plays critical roles in the synthesis of structural proteins and mucins, in intestinal barrier integrity, and in one-carbon metabolism. It also serves as a precursor for glycine and serine, both of which participate in the folate-mediated one-carbon pool pathway, essential for DNA methylation, nucleotide synthesis, and glutathione-mediated antioxidant defense.[22] Importantly, glycine and serine, both metabolic derivatives of threonine, are key players in numerous physiological pathways, and their depletion may

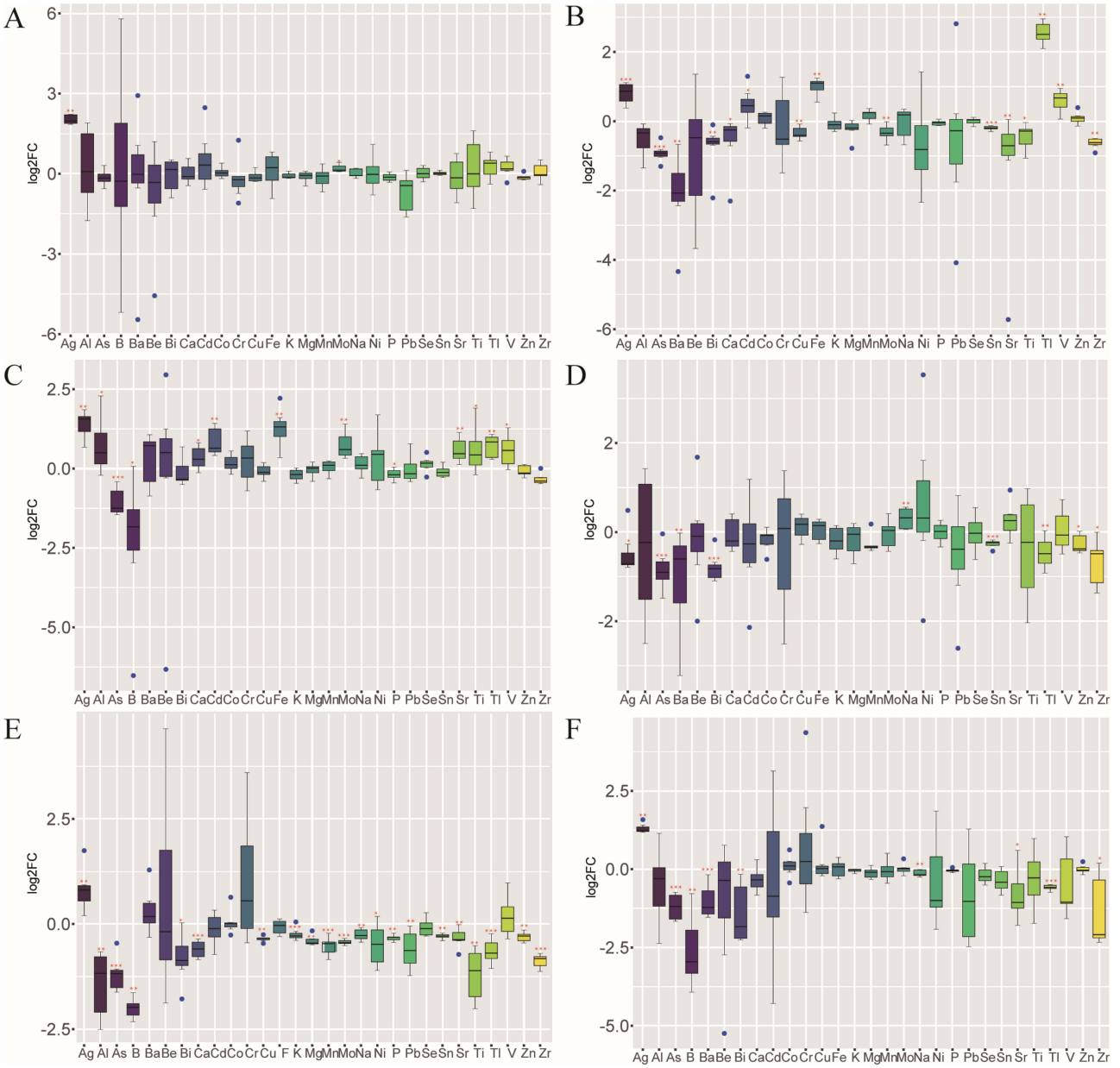

Figure 8 Contiune.

https://doi.org/10.2147/DDDT.S531720

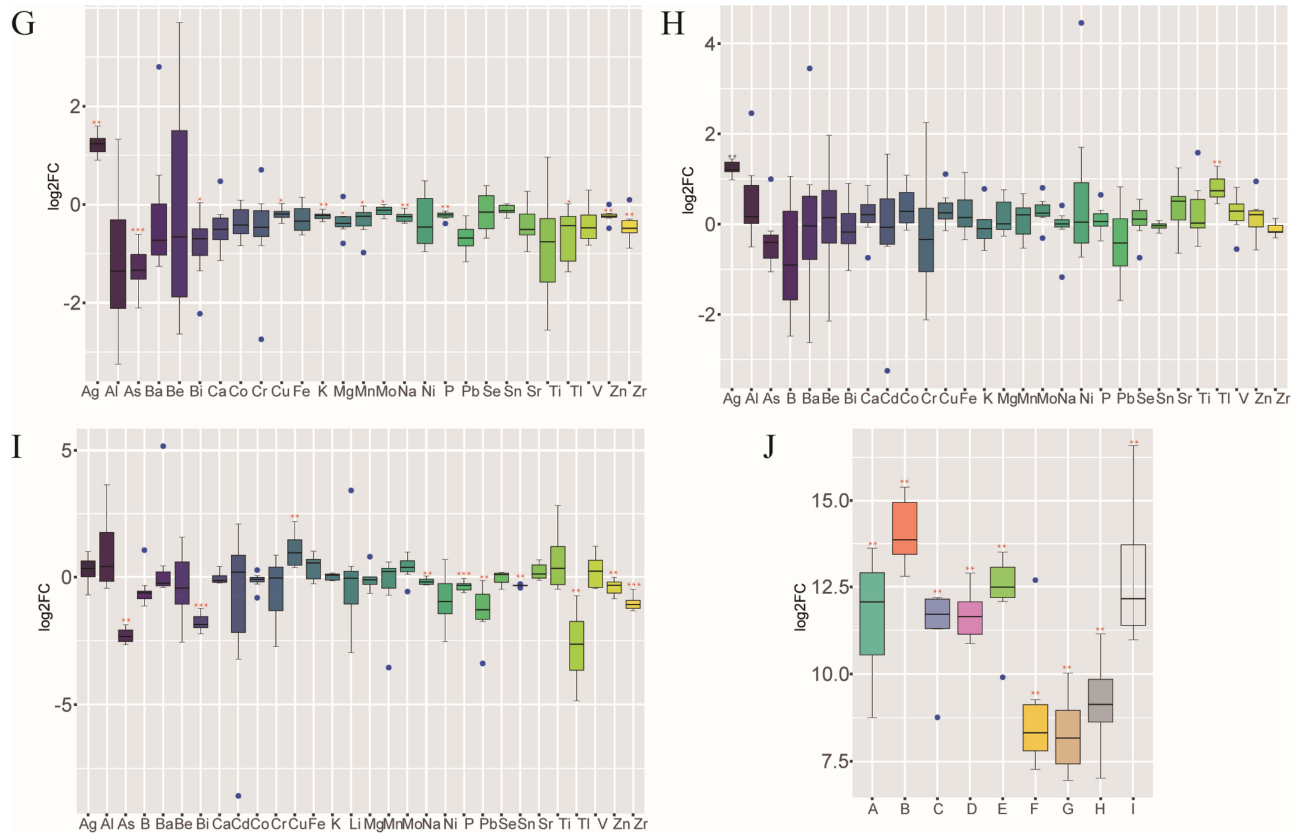

Figure 8 Elemental composition analysis across organs. (**A-I**) Log_2-transformed fold changes (log_2FC) of ion concentrations in cisplatin-treated versus control groups within individual organs: (**A**) Heart, (**B**) Liver, (**C**) Spleen, (**D**) Lung, (**E**) Kidney, (**F**) Cerebral cortex, (**G**) Hippocampus, (**H**) Brown fat, and (**I**) Serum. The y-axis represents log_2 (treated/control) for each ion, and the x-axis lists different ions. (**J**) Organ-specific distribution of platinum (Pt): The y-axis shows log_2(treated/control) of Pt concentration across organs. Statistical significance is indicated as follows: $p < 0.05$ (*), $p < 0.01$ (**), $p < 0.001$ (***).

amplify the downstream effects of threonine deficiency. Glycine, a critical inhibitory neurotransmitter in the central nervous system, regulates the excitability balance between neurons, thereby maintaining synaptic transmission and the stability of neural signals.[23] A reduction in glycine could impair the inhibitory regulation of the nervous system, thereby exacerbating cisplatin-induced neurotoxicity. Studies have demonstrated that glycine modulates the activity of NMDA receptors by synergizing with glutamate, influencing the opening of calcium ion channels, and subsequently regulating the release of neurotransmitters and synaptic function.[24] Simultaneously, the protective effect of glycine in the heart may be mediated by alleviating oxidative stress and inflammatory responses.[25] Glycine reduces the release of superoxide anion radicals (O_2^-) in the presence of NADPH, as well as decreases protein carbonylation and lipid peroxidation.[26] It can counteract fat accumulation and inflammatory responses, promoting fat metabolism and detoxification.[27] Studies have found that serine serves as a precursor to the neurotransmitter glycine and other neuromodulators. A reduction in serine may impair the nervous system's response to oxidative stress and nerve damage.[28] Additionally, serine serves as a key precursor for cell membrane synthesis, enhancing membrane function and promoting cardiomyocyte repair in heart disease.[29] In the liver, serine primarily participates in one-carbon metabolism. Serine deficiency can lead to liver metabolic disorders, disrupting lipid metabolism and glucose homeostasis.[30] Additionally, studies have shown that serine deficiency may impair spleen immune function, leading to a weakened immune response.[31] L-lysine is not only a critical amino acid for protein synthesis but also plays a significant role in immune response and cellular metabolic homeostasis. A decrease in L-lysine may result in immune system dysfunction, impairing immune cell activity and their response to external stimuli. Studies have shown that L-lysine regulates immune responses by influencing cytokine synthesis and secretion.[32] Cisplatin-induced reduction in L-lysine levels may be closely associated with immunotoxicity, thereby exacerbating structural and functional damage to the spleen and other immune organs. Studies have indicated that

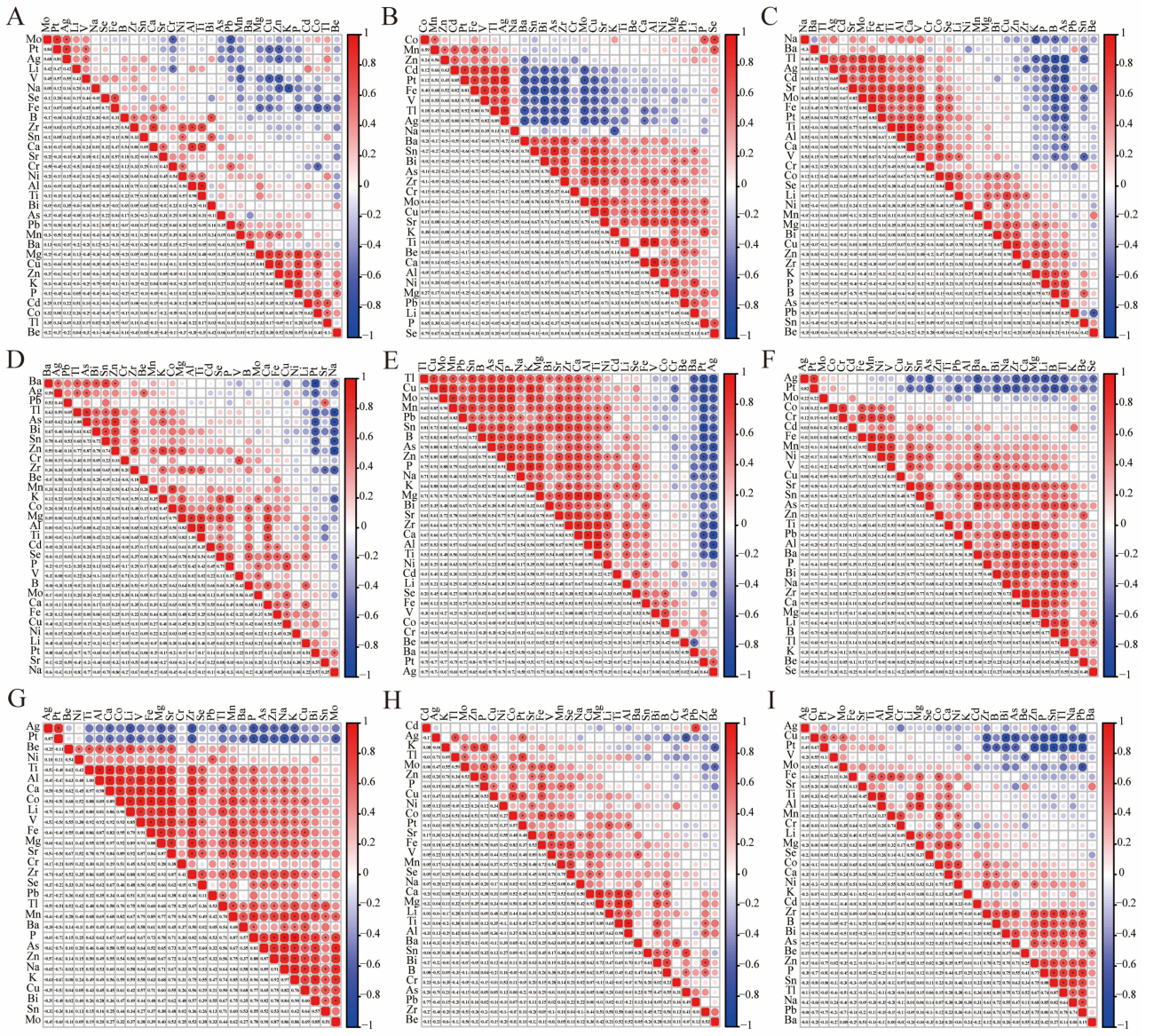

Figure 9 Correlation analysis of detected ions. The numbers in the cells of the lower triangle represent the Spearman correlation coefficients (r) for the corresponding elements. In the upper triangle, red and blue dots represent positive and negative correlations, respectively. The diameter of each dot is proportional to the magnitude of the correlation coefficient. (**A**) Heart, (**B**) Liver, (**C**) Spleen, (**D**) Lung, (**E**) Kidney, (**F**) Cerebral cortex, (**G**) Hippocampus,(**H**) Brown fat, and (**I**) Serum. Statistical significance is indicated as follows: $p < 0.05$ (*).

Glycyl-L-histidyl-L-lysine-Cu^{2+} attenuates cigarette smoke-induced pulmonary emphysema and inflammation by modulating the oxidative stress pathway.[33] As an essential amino acid, L-lysine is involved in protein synthesis and glucose metabolism in the liver; its deficiency can lead to liver metabolic disorders.

It is interesting that in this study, while the majority of amino acids exhibited a consistent decrease across multiple organs following cisplatin exposure, several key amino acids, including L-threonine, L-lysine, and serine, displayed increased levels in specific tissues such as the hippocampus and brown adipose tissue (BAT). These findings suggest that cisplatin-induced metabolic alterations are not uniform but exhibit strong organ specificity and potentially reflect tissue-specific compensatory or adaptive responses. Importantly, correlation analysis between metabolomics and ionomics data revealed that hippocampal L-threonine levels were positively correlated with Pt and Ag, and negatively correlated with As and Mo. These metal ions exhibited distinctive distribution patterns under cisplatin exposure: Pt and Ag were elevated, while essential elements such as As and Mo were significantly decreased in the hippocampus. Accumulation of

https://doi.org/10.2147/DDDT.S531720

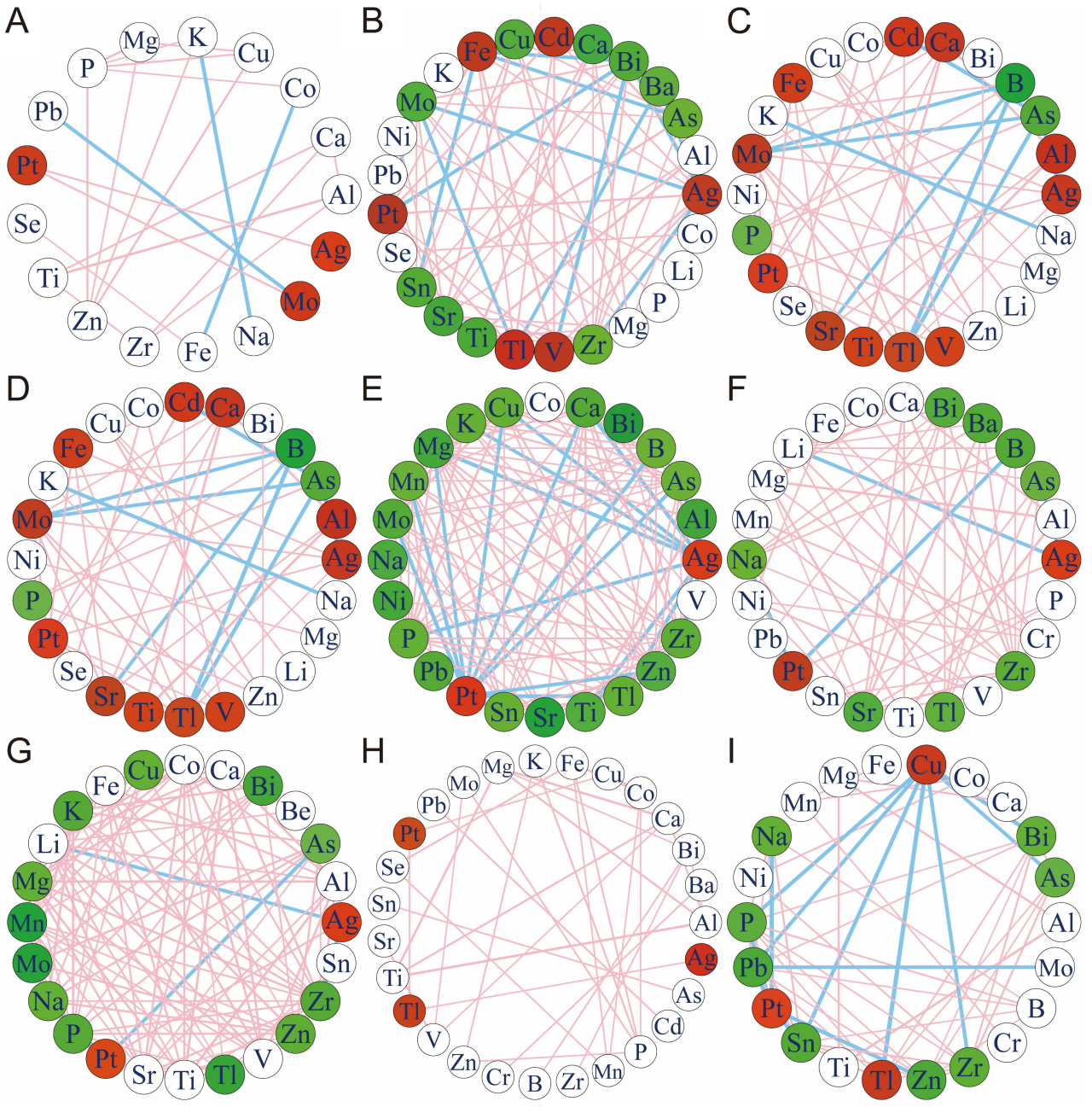

Figure 10 The elemental correlation network. Nodes represent individual ions. Differentially altered elements are highlighted in red (indicating an increase) and green (indicating a decrease). Only significant ion pairs with a Spearman correlation coefficient ($r > 0.7$) are connected by straight lines, with the line thickness proportional to the strength of the correlation. Red lines indicate positive correlations, whereas blue lines indicate negative correlations. (**A**) Heart, (**B**) Liver, (**C**) Spleen, (**D**) Lung, (**E**) Kidney, (**F**) Cerebral cortex, (**G**) Hippocampus, (**H**) Brown fat, and (**I**) Serum.

heavy metals like Pt and Ag has been associated with mitochondrial dysfunction and reactive oxygen species (ROS) generation,[34] while depletion of Mo and As may disrupt metalloenzyme functions and trace element homeostasis.[35] The increase in hippocampal threonine may reflect a compensatory metabolic shift in response to these ionic imbalances, possibly involving upregulated amino acid biosynthesis or impaired catabolic flux. Threonine is not only a proteinogenic amino acid but also involved in the synthesis of glycine and acetyl-CoA via threonine dehydrogenase, linking it to mitochondrial energy metabolism and redox status.[36] Serine, although not statistically significant in the hippocampus, was markedly elevated in BAT and showed positive correlations with Ag and Pt. As a central metabolite in one-carbon metabolism, phospholipid biosynthesis, and antioxidant defense, increased serine levels in BAT may reflect enhanced

Figure 11 Correlation analysis between metabolites and ions. The size of each circle represents the Spearman correlation coefficient (r), with red indicating positive correlations and blue indicating negative correlations. No circle is displayed when the P exceeds 0.05, indicating a lack of statistical significance. It represents statistical associations in fig, but deep biological interactions should be confirmed in further research. (**A**) Heart, (**B**) Liver, (**C**) Spleen, (**D**) Lung, (**E**) Kidney, (**F**) Cerebral cortex, (**G**) Hippocampus, (**H**) Brown fat, and (**I**) Serum.

https://doi.org/10.2147/DDDT.S531720

demand for redox buffering or membrane repair in response to oxidative and mitochondrial stress. Supporting this notion, BAT showed elevated levels of Ag, Tl, and Pt under cisplatin treatment, likely due to its high mitochondrial density and thermogenic activity, which may render it more susceptible to metal-induced toxicity. L-lysine, another amino acid increased in both the hippocampus and BAT, exhibited distinct organ-specific correlation profiles. In the hippocampus, lysine was positively correlated with Ag and Pt, but negatively correlated with Li and As; in BAT, it correlated positively with Ag and Tl. As an essential amino acid, lysine plays critical roles in protein turnover, epigenetic regulation, and mitochondrial fatty acid transport through its conversion to carnitine.[37] Elevated lysine levels may indicate increased demand for mitochondrial adaptation, or dysregulation of catabolic enzymes such as lysine-ketoglutarate reductase. Moreover, lysine accumulation might be involved in epigenetic remodeling under stress conditions via altered histone acetylation or methylation.[38] Metabolic pathway enrichment analysis further supports these findings. In the hippocampus, pathways significantly affected by cisplatin include alanine, aspartate and glutamate metabolism; pantothenate and CoA biosynthesis; and phenylalanine, tyrosine, and tryptophan biosynthesis. Disruption of CoA biosynthesis suggests mitochondrial dysfunction, while alterations in glutamate and aromatic amino acid metabolism may disturb excitatory neurotransmission.[38] These findings are in line with previous reports showing that cisplatin impacts central carbon metabolism, impairs neurotransmitter balance, and contributes to cognitive impairment and neurotoxicity.[39] Collectively, our integrative analysis suggests that cisplatin induces organ-specific and metal-associated amino acid alterations. The hippocampus, a critical region for learning and memory, appears particularly vulnerable due to the convergence of amino acid imbalance, heavy metal accumulation, and disrupted neurotransmitter pathways. These results shed light on potential mechanisms underlying cisplatin-induced neurotoxicity and identify candidate metabolic nodes, such as threonine and lysine metabolism, one-carbon pathways, and mitochondrial redox regulation, for future therapeutic intervention.

In our pathway enrichment analysis, phenylalanine, tyrosine and tryptophan biosynthesis emerged as a recurrently perturbed pathway in the heart, hippocampus, and brown adipose tissue (BAT), suggesting that aromatic amino acid metabolism is a shared target of cisplatin toxicity across both central and peripheral tissues. These amino acids are not only fundamental building blocks for protein synthesis but also serve as precursors for neurotransmitters such as dopamine, norepinephrine, and serotonin, implicating their dysregulation in both cognitive and systemic side effects of cisplatin.[40] The enrichment of phenylalanine metabolism and alanine, aspartate and glutamate metabolism in the hippocampus further supports the idea that neurotransmitter balance and excitatory signaling are key pathways affected by cisplatin exposure.[39] Additionally, pantothenate and CoA biosynthesis, enriched in the hippocampus and BAT, may reflect mitochondrial dysfunction and impaired energy metabolism, as CoA is essential for fatty acid oxidation and the TCA cycle.[41] Similar patterns have been observed in previous studies linking cisplatin to central carbon metabolism impairment and mitochondrial toxicity.[42] In the kidney, which is a primary target of cisplatin-induced injury, distinct pathways such as beta-alanine metabolism, taurine and hypotaurine metabolism, and arginine biosynthesis were affected. These changes likely reflect altered osmotic regulation, ammonia detoxification, and urea cycle activity in response to renal tubular stress. Overall, the recurrence of specific metabolic pathways across organs, particularly aromatic amino acid biosynthesis, suggests that cisplatin induces coordinated metabolic reprogramming. These alterations may underlie both the neurotoxic and nephrotoxic effects of the drug, highlighting potential metabolic targets for protective interventions.

Differential Ion Analysis

Our study found that excessive accumulation of cisplatin in the body significantly disrupts the ion balance in various organs of mice. The kidney is the primary target organ of cisplatin, and nephrotoxicity is one of the most common and severe side effects of its clinical application. Consistent with our experimental results, we observed the most prominent ion changes in the kidney. Cisplatin binds to sulfhydryl groups in renal tubular epithelial cells, forming toxic cisplatin-sulfhydryl complexes that cause damage to renal tubular cells, triggering oxidative stress and inflammatory responses.[43,44] Under cisplatin treatment, platinum accumulation is typically accompanied by a reduction in Cu and Zn levels. The copper-zinc form of SOD (Cu/Zn SOD) predominantly resides in the cytoplasm, and its activity depends on the involvement of copper ions. Copper serves as a catalyst at the SOD active site, facilitating the conversion of superoxide anions into oxygen and hydrogen peroxide. Copper deficiency leads to a decrease in SOD activity, weakening the antioxidant capacity of cells and increasing the risk of oxidative stress-induced damage. Previous studies have shown that cisplatin-induced oxidative stress

can disrupt copper homeostasis in human colon cancer cells, possibly through the copper transporter CTR1,[45] which further impairs the kidney's antioxidant defense capacity and exacerbates kidney damage. Furthermore, in the hippocampus, copper and Zinc reduction may impair neuronal antioxidant defenses, leading to the accumulation of free radicals and peroxides, resulting in nerve cell damage and triggering cognitive decline.[46,47]

We observed a notable accumulation of silver in multiple organs (including the heart, liver, spleen, kidney, cortex, hippocampus, and brown fat) following cisplatin treatment. This may reflect cisplatin's broad disruption of metal ion metabolism and cellular homeostasis. Mechanistically, cisplatin impairs renal excretion function by inducing oxidative stress, mitochondrial dysfunction, and apoptosis in tubular epithelial cells, facilitating systemic retention of metal ions such as silver.[48] Simultaneously, cisplatin-induced hepatic injury can reduce glutathione (GSH) levels and interfere with mitochondrial activity, further disrupting metal detoxification. These ionomic perturbations may contribute to alterations in multiple metabolic pathways observed in this study. For example, the upregulation of glutathione metabolism in the kidney suggests a compensatory response to metal-induced oxidative stress, while the observed changes in pantothenate and CoA biosynthesis in both the hippocampus and cerebral cortex may reflect mitochondrial damage and impaired energy metabolism linked to metal overload. Furthermore, silver accumulation may be partially mediated by the upregulation of metallothioneins (MTs), which bind metal ions such as silver and are transcriptionally regulated by inflammatory mediators (eg, NF-κB, TNF-α, IL-6).[48] These inflammatory pathways may also influence the observed metabolic changes in amino acid biosynthesis. Notably, the phenylalanine, tyrosine, and tryptophan biosynthesis pathway was consistently enriched across the heart, hippocampus, and brown adipose tissue, indicating a systemic dysregulation in aromatic amino acid metabolism. These amino acids are precursors for neurotransmitters and are highly sensitive to oxidative and inflammatory stress, which may be exacerbated by metal ion interference. Additionally, the cisplatin-silver interaction likely forms metabolically inert complexes through binding with intracellular thiol groups (eg, glutathione, cysteine), which may further disrupt cysteine-dependent metabolic processes such as glutathione synthesis, contributing to redox imbalance and altered energy metabolism. This is consistent with the observed changes in alanine, aspartate and glutamate metabolism, which were dysregulated in both the hippocampus and kidney-organs known for their metabolic vulnerability during oxidative damage.

In our research, we found significant reductions in As and Zr levels across multiple organs, while Tl levels exhibited both increases and decreases in different organs. As a well-known environmental toxin, arsenic is strongly associated with the onset of various health problems, particularly chronic diseases such as cancer, cardiovascular diseases, diabetes, and skin disorders. Research has demonstrated that arsenic inhibits antioxidant enzyme activity and activates oxidative stress pathways, leading to cellular damage and multi-organ dysfunction.[49] The reduction in arsenic levels observed in this study may be attributed to alterations in its metabolic pathways or to a reduced efficiency of detoxification mechanisms. These changes may influence arsenic bioavailability and toxicity within the body, further exacerbating organ damage. Zr is a poorly bioabsorbed metal, typically excreted via the kidneys. The decline in zirconium levels across organs may be linked to inefficiencies in its bioavailability or toxic effects within the body. The reduction in zirconium levels may be associated with alterations in its excretion mechanism, interactions with other metal ions, or modifications in metabolic pathways. The decrease in this metal reflects a potential suppression of the body's detoxification capacity to mitigate its toxicity. Tl changes are more complex. In this study, we observed an increase in thallium levels in the liver and spleen, while levels in other organs exhibited a decreasing trend. Thallium, a neurotoxic element, exerts significant effects on the nervous system and various organ functions. Studies have demonstrated that thallium exposure can affect neuronal excitability and nervous system function by interfering with ion permeability of the cell membrane and disrupting intracellular ion balance.[50] Additionally, thallium is hepatotoxic, interfering with liver detoxification functions and affecting its metabolic and detoxification processes. Thallium excretion is closely linked to its blood concentration, interactions with other metals, and its excretion mechanism. Thallium accumulation may be strongly associated with the onset of neurodegenerative diseases, such as Alzheimer's disease and Parkinson's disease, with its neurotoxic effects potentially serving as a key pathogenic factor.[51]

In our study, we observed a significant decrease in phosphorus content in the kidney, spleen, hippocampus, and heart following cisplatin treatment. Phosphorus metabolic dysregulation in the body may be closely associated with the oxidative stress and organ damage induced by cisplatin. A reduction in phosphorus levels may impact intracellular

energy metabolism, particularly the ATP synthesis process.[52] In the kidney, the reduction in phosphorus levels may be linked to cisplatin-induced tubular damage, which subsequently affects phosphorus absorption and excretion.[53] In the spleen, phosphorus depletion may be attributed to cisplatin's effects on immune function and metabolic balance through systemic oxidative stress. Phosphorus deficiency may inhibit immune cell activity and reduce the body's immune response, thereby compromising its defense against external stimuli and pathogens. Phosphorus is involved in ATP synthesis in nerve cells and is a critical factor in maintaining neuronal function.[52] Additionally, phosphorus deficiency may impair calcium absorption, disrupt calcium metabolism, and increase the risk of osteomalacia.[54] Interestingly, phosphorus can modulate the activity of antioxidant enzymes, such as glutathione peroxidase, which rely on copper and zinc as cofactors to scavenge free radicals in cells. Phosphorus deficiency may reduce antioxidant capacity, thereby exacerbating oxidative stress resulting from copper or zinc deficiency. Similarly, phosphorus deficiency may disrupt iron metabolism by impairing the iron absorption mechanism, potentially leading to anemia.[55]

Integrated metabolomic and ionomic data revealed significant correlations between metabolites and metal ions in the kidney following cisplatin treatment, reflecting the complex mechanisms underlying its toxicity. In the kidney, L-alanine exhibited a strong positive correlation with Cu and Mg ($r > 0.8$, $P < 0.05$), while showing a negative association with Ag and Pt. These findings suggest that cisplatin may reorganize the renal metabolic network by disrupting metal ion homeostasis and modulating metal-dependent enzymatic activities. The correlation of L-alanine with Cu and Mg indicates a potential association between this amino acid and the distribution of these metal ions in the kidney. Copper is commonly involved in redox-related enzymatic systems, such as cytochrome coxidase and Cu/Zn-superoxide dismutase (SOD1), which are implicated in reactive oxygen species (ROS) detoxification and mitochondrial energy metabolism under stress conditions.[56] Magnesium is broadly required for the structural and functional integrity of ATP-dependent enzymes, including mitochondrial ATP synthase, and is frequently linked to cellular responses during oxidative stress.[57] In contrast, the observed negative correlation between L-alanine and Ag/Pt may be related to the altered ionic environment induced by cisplatin treatment. Both silver and platinum are known to interact with thiol-containing proteins and mitochondrial components, which have been reported to influence redox balance and enzymatic activities.[58] These findings suggest that L-alanine levels may reflect shifts in renal metal ion homeostasis and associated metabolic processes following cisplatin exposure. Additionally, in the hippocampus, Ag levels were significantly positively correlated with several amino acids, including L-alanine, L-leucine, L-lysine, L-threonine, L-proline, and L-phenylalanine. These correlations could indicate possible links between silver accumulation and alterations in neuronal amino acid metabolism or transport. Previous studies have suggested that silver may affect neuronal function by enhancing oxidative stress, interfering with amino acid transporters, or affecting membrane stability. Such alterations may contribute to the neurotoxic effects observed following cisplatin treatment, including potential deficits in hippocampus-dependent memory and cognitive function. As a result, these findings support an association between cisplatin-induced metabolic perturbations and disrupted metal ion homeostasis, providing a framework for further investigation into the systemic mechanisms of cisplatin toxicity and its modulation.

Conclusion

This study systematically explored the effects of cisplatin treatment on the metabolome and ionome of various organ tissues in mice by combining gas chromatography-mass spectrometry (GC-MS) and inductively coupled plasma mass spectrometry (ICP-MS). The goal was to investigate the mechanisms of cisplatin toxicity across multiple organs and to generate hypotheses regarding candidate therapeutic targets for mitigating its toxic side effects in clinical settings. Through comprehensive analysis of differential metabolites and metal ions, this study found that cisplatin treatment significantly altered the levels of several key metabolites, including Phenylalanine, tyrosine and tryptophan biosynthesis, Alanine, aspartate and glutamate metabolism, Pantothenate and CoA biosynthesis. Furthermore, significant fluctuations in metal ions such as Ag, Cu, Zn, Fe, and Mg highlighted the critical role of metal ions in cisplatin-induced toxicity. Previous studies have indicated that cisplatin may cause organ damage through mechanisms such as oxidative stress, inflammatory responses, disruption of cell signal transduction, and impairment of energy metabolism. The integrated analysis of metabolomics and ionomics identified multi-level alterations in cellular energy metabolism and ion homeostasis following cisplatin exposure. These results provide a basis for further exploration of potential biological processes

associated with cisplatin-related toxicity and its modulation. Although this study utilized GC-MS and ICP-MS techniques for metabolic and ionomic profiling, several limitations should be acknowledged. First, GC-MS is suitable for detecting small, volatile, and semi-volatile metabolites, but cannot effectively capture macromolecules or highly polar compounds. Second, the sample size and diversity of organ types analyzed were relatively limited, potentially affecting the generalizability of the findings. Third, although body weight loss and histopathological assessments indicated cisplatin-induced toxicity, standard biochemical markers such as serum blood urea nitrogen and creatinine for evaluating renal function, as well as alanine aminotransferase and aspartate aminotransferase for assessing liver function, were not measured. The lack of these quantitative indicators may reduce the precision of toxicity assessment. Future investigations should integrate these biomarkers to improve the rigor and translational relevance of the results.

Overall, this study comprehensively investigated the toxic effects of cisplatin on multiple organs from the dual perspectives of metabolism and ionomics, providing essential data to elucidate its toxic mechanisms across various organs. Future studies could further elucidate the organ toxicity of cisplatin by integrating genomic, transcriptomic, and metabolomic data, combining multi-omics platforms, and utilizing larger sample sizes. The application of advanced data analysis techniques, particularly machine learning and network analysis methods, is expected to provide novel insights into the specific responses of cisplatin in different organs, thereby aiding the development of precise toxicity intervention strategies. Studies have shown that the deficiency or abnormal increase of certain key metabolites or elements significantly influences the toxicity of cisplatin, with these changes exacerbating cisplatin-induced toxicity through mechanisms such as oxidative stress and inflammatory signaling pathways. Therefore, supplementation or reduction of these key metabolites or elements may mitigate cisplatin-induced toxic reactions.

Data Sharing Statement

The datasets used and/or analyzed during the current study are available from the corresponding author on reasonable request.

Ethics Approval and Consent to Participate

This study adhered to the guidelines for the care and use of experimental animals issued by the State Science and Technology Commission of the People's Republic of China, and the research protocol was approved by the institutional ethics committee (approval number: JNRM-2024-DW-158).

Author Contributions

All authors made a significant contribution to the work reported, whether that is in the conception, study design, execution, acquisition of data, analysis and interpretation, or in all these areas; took part in drafting, revising or critically reviewing the article; gave final approval of the version to be published; have agreed on the journal to which the article has been submitted; and agree to be accountable for all aspects of the work. *RS* and QX contributed equally to this work as co-first authors. YZZ and PJ are co-corresponding authors and jointly designed the study.

Funding

This study was supported by the National Natural Science Foundation of China (No. 82373585), the Natural Science Foundation of Shandong Province (No. ZR2022MH007), and the Development Fund Project of the Affiliated Hospital of Xuzhou Medical University (No. XYFY202417).

Disclosure

The authors declare that they have no known competing financial interests or personal relationships that could have appeared to influence the work reported in this paper.

References

1. Rodler E, Sharma P, Barlow WE, et al. Cisplatin with veliparib or placebo in metastatic triple-negative breast cancer and BRCA mutation-associated breast cancer (S1416): a randomised, double-blind, placebo-controlled, phase 2 trial. *Lancet Oncol*. 2023;24(2):162–174. doi:10.1016/S1470-2045(22)00739-2

2. Siegel RL, Miller KD, Fuchs HE, Jemal A. Cancer statistics, 2022. *CA Cancer J Clin*. 2022;72(1):7–33. doi:10.3322/caac.21708
3. Raudenska M, Balvan J, Fojtu M, Gumulec J, Masarik M. Unexpected therapeutic effects of cisplatin. *Metallomics*. 2019;11(7):1182–1199. doi:10.1039/c9mt00049f
4. Wu CK, Shiu JL, Wu CL, et al. APLF facilitates interstrand DNA crosslink repair and replication fork protection to confer cisplatin resistance. *Nucleic Acids Res*. 2024;52(10):5676–5697. doi:10.1093/nar/gkae211
5. Elmorsy EA, Saber S, Hamad RS, et al. Advances in understanding cisplatin-induced toxicity: molecular mechanisms and protective strategies. *Eur J Pharm Sci*. 2024;203:106939. doi:10.1016/j.ejps.2024.106939
6. Liao JC, Li CY, Teng FM, et al. Integrated analysis of comprehensive metabolomics and network pharmacology to reveal the mechanisms of abelmoschus manihot (L.) medik. in the treatment of cisplatin-induced chronic kidney disease. *Front Pharmacol*. 2022;13:1064498. doi:10.3389/fphar.2022.1064498
7. Michalke B. Editorial on the occasion of the 25th anniversary of the journal of trace elements in medicine and biology. *J Trace Elem Med Biol*. 2011;25(1):1–2. doi:10.1016/j.jtemb.2010.12.001
8. Jiang C, Zhao QQ, Gao Q, et al. Diagnostic potential of ionomic profile in the plasma of cervical cancer patients receiving neoadjuvant chemoradiotherapy. *J Trace Elem Med Biol*. 2020;57:68–74. doi:10.1016/j.jtemb.2019.09.009
9. Baima G, Iaderosa G, Corana M, et al. Macro and trace elements signature of periodontitis in saliva: a systematic review with quality assessment of ionomics studies. *J Periodontal Res*. 2022;57(1):30–40. doi:10.1111/jre.12956
10. Lim SY, Dayal H, Seah SJ, et al. Plasma metallomics reveals potential biomarkers and insights into the ambivalent associations of elements with acute myocardial infarction. *J Trace Elem Med Biol*. 2023;77:127148. doi:10.1016/j.jtemb.2023.127148
11. Zhou R, Fu W, Vasylyev D, Waxman SG, Liu CJ. Ion channels in osteoarthritis: emerging roles and potential targets. *Nat Rev Rheumatol*. 2024;20(9):545–564. doi:10.1038/s41584-024-01146-0
12. Chen LL, Fan YG, Zhao LX, Zhang Q, Wang ZY. The metal ion hypothesis of Alzheimer's disease and the anti-neuroinflammatory effect of metal chelators. *Bioorg Chem*. 2023;131:106301. doi:10.1016/j.bioorg.2022.106301
13. Naseem I, Hassan I, Alhazza IM, Chibber S. Protective effect of riboflavin on cisplatin induced toxicities: a gender-dependent study. *J Trace Elem Med Biol*. 2015;29:303–314. doi:10.1016/j.jtemb.2014.08.003
14. Shen Z, Lin J, Teng J, et al. Association of urinary ionomic profiles and acute kidney injury and mortality in patients after cardiac surgery. *J Thorac Cardiovasc Surg*. 2020;159(3):918–26.e5. doi:10.1016/j.jtcvs.2019.02.095
15. Groehler A, Maratova A, Dao NM, Mahkmut A, Schärer OD. Development of comprehensive ultraperformance liquid chromatography-high-resolution mass spectrometry assays to quantitate cisplatin-induced DNA-DNA cross-links. *Chem Res Toxicol*. 2023;36(6):822–837. doi:10.1021/acs.chemrestox.2c00308
16. Chandra S. Quantitative imaging of chemical composition in single cells by secondary ion mass spectrometry: cisplatin affects calcium stores in renal epithelial cells. *Methods Mol Biol*. 2010;656:113–130.
17. Yu B, Jin L, Yao X, et al. TRPM2 protects against cisplatin-induced acute kidney injury and mitochondrial dysfunction via modulating autophagy. *Theranostics*. 2023;13(13):4356–4375. doi:10.7150/thno.84655
18. Sung CYW, Hayase N, Yuen PST, et al. Macrophage depletion protects against cisplatin-induced ototoxicity and nephrotoxicity. *Sci Adv*. 2024;10(30):eadk9878. doi:10.1126/sciadv.adk9878
19. Tan Y, Li J, Zhao G, et al. Metabolic reprogramming from glycolysis to fatty acid uptake and beta-oxidation in platinum-resistant cancer cells. *Nat Commun*. 2022;13(1):4554. doi:10.1038/s41467-022-32101-w
20. Aladaileh SH, Al-Swailmi FK, Abukhalil MH, Ahmeda AF, Mahmoud AM. Punicalagin prevents cisplatin-induced nephrotoxicity by attenuating oxidative stress, inflammatory response, and apoptosis in rats. *Life Sci*. 2021;286:120071. doi:10.1016/j.lfs.2021.120071
21. Pervushin NV, Yapryntseva MA, Panteleev MA, Zhivotovsky B, Kopeina GS. Cisplatin resistance and metabolism: simplification of complexity. *Cancers*. 2024;16(17):3082. doi:10.3390/cancers16173082
22. Jog RM. *Hormonal Regulation of Glycine Decarboxylase and Its Metabolic Outcomes*. Wayne State University; 2020.
23. Alger B, Le Beau F. Physiology of the GABA and glycine systems. In: *Pharmacology of GABA and Glycine Neurotransmission*. Springer; 2001:3–76.
24. Niciu MJ, Kelmendi B, Sanacora G. Overview of glutamatergic neurotransmission in the nervous system. *Pharmacol Biochem Behav*. 2012;100(4):656–664. doi:10.1016/j.pbb.2011.08.008
25. Pérez-Torres I, María Zuniga-Munoz A, Guarner-Lans V. Beneficial effects of the amino acid glycine. *Mini Rev Med Chem*. 2017;17(1):15–32. doi:10.2174/1389557516666160609081602
26. Ruiz-Ramírez A, Ortiz-Balderas E, Cardozo-Saldaña G, Diaz-Diaz E, El-Hafidi M. Glycine restores glutathione and protects against oxidative stress in vascular tissue from sucrose-fed rats. *Clin Sci*. 2014;126(1):19–29. doi:10.1042/CS20130164
27. Haddad JJ, Harb HL. l-γ-Glutamyl-l-cysteinyl-glycine (glutathione; GSH) and GSH-related enzymes in the regulation of pro-and anti-inflammatory cytokines: a signaling transcriptional scenario for redox (y) immunologic sensor (s)? *Mol Immunol*. 2005;42(9):987–1014. doi:10.1016/j.molimm.2004.09.029
28. Maiese K, Chong ZZ, Wang S, Shang YC. Oxidant stress and signal transduction in the nervous system with the PI 3-K, Akt, and mTOR cascade. *Int J Mol Sci*. 2012;13(11):13830–13866. doi:10.3390/ijms131113830
29. Cheng X, Wang K, Zhao Y, Wang K. Research progress on post-translational modification of proteins and cardiovascular diseases. *Cell Death Discovery*. 2023;9(1):275. doi:10.1038/s41420-023-01560-5
30. Pan S, Fan M, Liu Z, Li X, Wang H. Serine, glycine and one-carbon metabolism in cancer. *Int J Oncol*. 2020;58(2):158–170. doi:10.3892/ijo.2020.5158
31. Li P, Yin Y-L, Li D, Kim SW, Wu G. Amino acids and immune function. *Br J Nutr*. 2007;98(2):237–252. doi:10.1017/S000711450769936X
32. Hu Y, Feng L, Jiang W, et al. Lysine deficiency impaired growth performance and immune response and aggravated inflammatory response of the skin, spleen and head kidney in grown-up grass carp (Ctenopharyngodon idella). *Animal Nutrition*. 2021;7(2):556–568. doi:10.1016/j.aninu.2020.07.009
33. Zhang Q, Yan L, Lu J, Zhou X. Glycyl-L-histidyl-L-lysine-Cu2+ attenuates cigarette smoke-induced pulmonary emphysema and inflammation by reducing oxidative stress pathway. *Front Mol Biosci*. 2022;9:925700. doi:10.3389/fmolb.2022.925700
34. Sun Q, Li Y, Shi L, et al. Heavy metals induced mitochondrial dysfunction in animals: molecular mechanism of toxicity. *Toxicology*. 2022;469:153136. doi:10.1016/j.tox.2022.153136
35. Teschke R. Aluminum, arsenic, beryllium, cadmium, chromium, cobalt, copper, iron, lead, mercury, molybdenum, nickel, platinum, thallium, titanium, vanadium, and zinc: molecular aspects in experimental liver injury. *Int J Mol Sci*. 2022;23(20):12213. doi:10.3390/ijms232012213

36. Malinovsky A. Why threonine is an essential amino acid in mammals and birds: studies at the enzyme level. *Biochemistry*. 2018;83(7):795–799. doi:10.1134/S0006297918070039
37. Xiang F, Zhang Z, Xie J, et al. Comprehensive review of the expanding roles of the carnitine pool in metabolic physiology: beyond fatty acid oxidation. *J Transl Med*. 2025;23(1):324. doi:10.1186/s12967-025-06341-5
38. Ali I, Conrad RJ, Verdin E, Ott M. Lysine acetylation goes global: from epigenetics to metabolism and therapeutics. *Chem Rev*. 2018;118(3):1216–1252. doi:10.1021/acs.chemrev.7b00181
39. Alhowail AH. Cisplatin induces hippocampal neurotoxicity and cognitive impairment in rats through neuroinflammation, oxidative stress, and overexpression of glutamatergic receptors mRNA. *Front Pharmacol*. 2025;16:1592511. doi:10.3389/fphar.2025.1592511
40. Ghallab YK, Elassal OS. Biochemical and neuropharmacology of psychiatric disorders. In: *Nutrition and Psychiatric Disorders: An Evidence-Based Approach to Understanding the Diet-Brain Connection*. Springer; 2024:25–47.
41. Moiseenok AG, Kanunnikova NP. Brain CoA and acetyl CoA metabolism in mechanisms of neurodegeneration. *Biochemistry*. 2023;88(4):466–480. doi:10.1134/S000629792304003X
42. Yu W, Chen Y, Dubrulle J, et al. Cisplatin generates oxidative stress which is accompanied by rapid shifts in central carbon metabolism. *Sci Rep*. 2018;8(1):4306.
43. Jiang H, Hong Y, Fan G. Bismuth reduces cisplatin-induced nephrotoxicity via enhancing glutathione conjugation and vesicular transport. *Front Pharmacol*. 2022;13:887876. doi:10.3389/fphar.2022.887876
44. Manohar S, Leung N. Cisplatin nephrotoxicity: a review of the literature. *J Nephrol*. 2018;31(1):15–25. doi:10.1007/s40620-017-0392-z
45. Akerfeldt MC, Tran CM-N, Shen C, Hambley TW, New EJ. Interactions of cisplatin and the copper transporter CTR1 in human colon cancer cells. *J Biol Inorg Chem*. 2017;22(5):765–774. doi:10.1007/s00775-017-1467-y
46. Mezzaroba L, Alfieri DF, Simão ANC, Reiche EMV. The role of zinc, copper, manganese and iron in neurodegenerative diseases. *Neurotoxicology*. 2019;74:230–241. doi:10.1016/j.neuro.2019.07.007
47. Gromadzka G, Tarnacka B, Flaga A, Adamczyk A. Copper dyshomeostasis in neurodegenerative diseases—therapeutic implications. *Int J Mol Sci*. 2020;21(23):9259.
48. Davoudi M, Jadidi Y, Moayedi K, Farrokhi V, Afrisham R. Ameliorative impacts of polymeric and metallic nanoparticles on cisplatin-induced nephrotoxicity: a 2011–2022 review. *J Nanobiotechnol*. 2022;20(1):504.
49. Xu G, Gu Y, Yan N, Li Y, Sun L, Li B. Curcumin functions as an anti-inflammatory and antioxidant agent on arsenic-induced hepatic and kidney injury by inhibiting MAPKs/NF-κB and activating Nrf2 pathways. *Environ Toxicol*. 2021;36(11):2161–2173. doi:10.1002/tox.23330
50. Nava-Ruíz C, Méndez-Armenta M. Cadmium, lead, thallium: occurrence, neurotoxicity and histopathological changes of the nervous system. Pollutant diseases, remediation and recycling. 2013;321–349.
51. Caito S, Aschner M. Neurotoxicity of metals. *Handbook Clin Neurol*. 2015;131:169–189.
52. Bonora M, Patergnani S, Rimessi A, et al. ATP synthesis and storage. *Purinergic Signalling*. 2012;8(3):343–357. doi:10.1007/s11302-012-9305-8
53. Tang C, Livingston MJ, Safirstein R, Dong Z. Cisplatin nephrotoxicity: new insights and therapeutic implications. *Nat Rev Nephrol*. 2023;19(1):53–72. doi:10.1038/s41581-022-00631-7
54. Bartl R. Calcium and Vitamin D Deficiency and Osteomalacia. In: *Osteoporosis in Clinical Practice*. Springer; 2023:77–90.
55. Kalantar-Zadeh K, Ganz T, Trumbo H, Seid MH, Goodnough LT, Levine MA. Parenteral iron therapy and phosphorus homeostasis: a review. *Am J Hematol*. 2021;96(5):606–616. doi:10.1002/ajh.26100
56. Jomova K, Alomar SY, Valko R, Nepovimova E, Kuca K, Valko M. The role of redox-active iron, copper, manganese, and redox-inactive zinc in toxicity, oxidative stress, and human diseases. *EXCLI J*. 2025;24:880–954.
57. Fatima G, Dzupina A, Alhmadi HB, et al. Magnesium matters: a comprehensive review of its vital role in health and diseases. *Cureus*. 2024;16(10).
58. Esmailzadeh F, Taheri-Ledari R, Salehi MM, et al. Bonding states of gold/silver plasmonic nanostructures and sulfur-containing active biological ingredients in biomedical applications: a review. *Phys Chem Chem Phys*. 2024;26(23):16407–16437. doi:10.1039/D3CP04131J